

1 **Variations in the chemical composition of the submicron aerosol and in the**
2 **sources of the organic fraction at a regional background site of the Po Valley**
3 **(Italy)**

4
5 **Michael Bressi¹, Fabrizia Cavalli¹, Claudio A. Belis¹, Jean-Philippe Putaud¹, Roman Fröhlich², Sebastiao**
6 **Martins dos Santos¹, Ettore Petralia³, André S. H. Prévôt², Massimo Berico³, Antonella Malaguti³ and**
7 **Francesco Canonaco²**

8
9 ¹European Commission, Joint Research Centre, Institute for Environment and Sustainability, Air and
10 Climate Unit, Via Enrico Fermi 2749, Ispra (VA) 21027, Italy.

11 ²Paul Scherrer Institute, Laboratory of Atmospheric Chemistry, Villigen 5232, Switzerland.

12 ³Italian National Agency for New Technologies, Energy and Sustainable Economic Development (ENEA),
13 Via Martiri di Monte Sole 4, Bologna 40129, Italy.

14
15 Correspondence to:

16 michael.s.bressi@gmail.com, claudio.belis@jrc.ec.europa.eu, fabrizia.cavalli@jrc.ec.europa.eu

17
18 **Abstract**

19 Fine particulate matter (PM) levels and resulting impacts on human health are in the Po Valley (Italy)
20 among the highest in Europe. To build effective PM abatement strategies, it is necessary to characterize
21 fine PM chemical composition, sources and atmospheric processes on long time scales (>months), with
22 short time resolution (<day), and with particular emphasis on the predominant organic fraction.
23 Although previous studies have been conducted in this region, none of them addressed all these aspects
24 together. For the first time in the Po Valley, we investigate the chemical composition of non-refractory
25 submicron PM (NR-PM₁) with a time-resolution of 30 minutes at the regional background site of Ispra
26 during one full year, using an Aerosol Chemical Speciation Monitor (ACSM) under the most up-to-date
27 and stringent quality assurance protocol. The identification of the main components of the organic
28 fraction is made using the Multilinear-Engine 2 algorithm implemented within the latest version of the
29 SoFi toolkit. In addition, with a view of a potential implementation of ACSM measurements in European
30 air quality networks as a replacement of traditional filter-based techniques, parallel multiple off-line
31 analyses were carried out to assess the performance of the ACSM in the determination of PM chemical

32 species regulated by Air Quality Directives. The annual NR-PM₁ level monitored at the study site (14.2
33 µg/m³) is among the highest in Europe, and is even comparable to levels reported in urban areas like
34 New York City and Tokyo. On the annual basis, submicron particles are primarily composed of organic
35 aerosol (OA, 58% of NR-PM₁). This fraction was apportioned into oxygenated OA (OOA, 66%),
36 hydrocarbon-like OA (HOA, 11% of OA), and biomass burning OA (BBOA, 23%). Among the primary
37 sources of OA, biomass burning (23%) is thus bigger than fossil fuel combustion (11%). Significant
38 contributions of aged secondary organic aerosol (OOA) are observed throughout the year. The
39 unexpectedly high degree of oxygenation estimated during wintertime is probably due to the
40 contribution of secondary BBOA and the enhancement of aqueous phase production of OOA during cold
41 months. BBOA and nitrate are the only components of which contributions increase with the NR-PM₁
42 levels. Therefore, biomass burning and NO_x emission reductions would be particularly efficient in
43 limiting submicron aerosol pollution events. Abatement strategies conducted during cold seasons
44 appear to be more efficient than annual-based policies. In a broader context, further studies using high-
45 time resolution analytical techniques on a long-term basis for the characterization of fine aerosol should
46 help better shape our future air quality policies, which constantly need refinement.

47

48 1. Introduction

49 The Po Valley region - located in northern Italy - is amongst the most polluted areas in Europe (van
50 Donkelaar et al., 2010; EEA, 2013). Annual PM_{2.5} (particulate matter with an aerodynamic diameter
51 below 2.5 µm) mean concentrations can significantly exceed the European PM_{2.5} annual limit value (25
52 µg/m³ in 2015, European Directive 2008/50/EC) and the recommendations of the World Health
53 Organization (PM_{2.5} annual average of 10 µg/m³; WHO, 2006) at urban (e.g. Bologna, 35.8 µg/m³) and
54 regional background sites (e.g. Ispra, 32.2 µg/m³; Putaud et al., 2010). Consequently, PM_{2.5} impacts on
55 human health are among the most severe in Europe (EC, 2005), while impacts on the local radiative
56 forcing are substantial (Clerici and Mélin, 2008; Ferrero et al., 2014; Putaud et al., 2014b). Effective PM
57 abatement strategies are thus needed in the Po Valley and require an in-depth knowledge of the
58 chemical composition of fine PM, to quantify its sources and the atmospheric processes leading to its
59 secondary formation.

60 In this region, high levels of fine aerosol are mostly due to the conjunction of i) high pollutant
61 emissions related to industrial, transport, biomass burning and agricultural activities - the Po river basin
62 hosting 37% of the Italian industries, 55% of the livestock and contributing 35% of the Italian agricultural
63 production (WMO et al., 2012) - and ii) the specific geography and topography of this area - a flat basin

64 surrounded by the Alps and Apennine Mountains dominated by weak winds that favour the
65 accumulation of pollutants (Decesari et al., 2014; Kukkonen et al., 2005; Pernigotti et al., 2012). As a
66 consequence, PM levels are not only high in urban areas but also at regional and rural background sites,
67 which are key locations for investigating air pollution due to their distance from local sources and local
68 phenomena. Measurements of fine PM mass and chemical composition at rural background sites are in
69 addition specifically required in the current European Directive on air quality (EU, 2008).

70 Previous studies have investigated the properties of fine aerosols at regional and rural
71 background sites of the Po valley region, including their chemical characteristics (e.g. Carbone et al.,
72 2014; Putaud et al., 2002, 2010; Saarikoski et al., 2012), and their main sources (Belis et al., 2013;
73 Gilardoni et al., 2011; Larsen et al., 2012; Perrone et al., 2012). Fine aerosols are primarily made of
74 organics (30-80% of fine PM mass, depending on the site and season studied), followed by ammonium
75 nitrate and ammonium sulfate. Their main sources are fossil fuel, biomass burning and biogenic
76 emissions to name a few. In addition, studies based on aerosol mass spectrometer measurements have
77 been conducted in the Po valley, with the aim of characterizing specific phenomena (e.g. fog events,
78 cooking aerosols) or seasons (Dall'Osto et al., 2015; Decesari et al., 2014; Gilardoni et al., 2014;
79 Saarikoski et al., 2012). In studies dealing with long time-series (entire season or year), the chemical
80 composition of fine aerosol is generally measured with a relatively low time resolution (typically 24
81 hours), thus preventing from studying its diurnal variation and short-lived chemical-physical processes.
82 When documented with higher time-resolutions (1 hour or less), aerosol chemical composition and its
83 sources are usually characterized for intensive campaigns of a few weeks only, hence not suitable to
84 depict the seasonal or yearly air quality situation. In addition, the complexity of the fine organic fraction
85 (e.g. Jimenez et al., 2009) requires state-of-the-art analytical and source apportionment (SA) techniques
86 to identify organic aerosol chemical properties and sources.

87 The recently developed Aerosol Chemical Speciation Monitor (ACSM, Aerodyne Research Inc.,
88 Ng et al., 2011a) is suitable to fill these gaps by providing the chemical composition of non-refractory
89 submicron aerosols (NR-PM₁) with a time resolution of 30 min, while operating on long time scales. Even
90 though promising results have been recently reported (e.g. Budisulistiorini et al., 2014; Canonaco et al.,
91 2013, 2015; Minguillón et al., 2015; Ng et al., 2011a; Petit et al., 2015; Ripoll et al., 2015; Sun et al.,
92 2012), this technique is still novel and requires additional field deployment to test its consistency with
93 independent methods for the monitoring of fine PM chemistry (e.g. filter measurements). In addition,
94 information on the accuracy of this technique is of paramount importance given the growing number of
95 ACSMs in Europe and the necessity to build a network of quality assured and harmonized instruments

96 for comparability of results – at present about 20 ACSMs are in operation in Europe
97 (<http://www.psi.ch/acsm-stations/overview-full-period>) within the frame of the EU ACTRIS network
98 (Aerosols, Clouds, and Traces gases Research InfraStructure, <http://www.actris.eu/>). Moreover, by using
99 receptor models, the apportionment of organic aerosol (OA) into its major components - hydrocarbon-
100 like (HOA), biomass burning (BBOA) and oxygenated OA (OOA) - can be performed (Lanz et al., 2007;
101 Zhang et al., 2011 and references therein).

102 In this study, we used an ACSM during one year with a 30-min time-resolution at a regional
103 background site of the Po Valley and performed subsequent SA analyses with the aim of: i) describing
104 the high time resolved chemical composition of NR-PM₁ on a long time-scale, to better understand the
105 physicochemical processes driving its temporal variations, ii) apportioning the organic fraction into its
106 main sources, iii) identifying PM abatement strategies to efficiently reduce NR-PM₁ pollution events at
107 regional background areas of the Po valley, and iv) assessing the atmospheric consistency of ACSM
108 measurements when compared to independent analytical methods, to evaluate its possible
109 implementation in future European Air Quality networks.

110

111 2. Material and methods

112 2.1. Sampling site

113 Measurements were conducted at the European Commission – Joint Research Centre (EC-JRC) Ispra site
114 (45°48'N, 8°38'E, 217 m a.s.l.; Fig. S1), which is part of the European Monitoring and Evaluation
115 Programme (EMEP) measurement network ([http://www.nilu.no/projects/ccc/](http://www.nilu.no/projects/ccc/sitedescriptions/it/index.html)
116 [sitedescriptions/it/index.html](http://www.nilu.no/projects/ccc/sitedescriptions/it/index.html)) and the Global Atmosphere Watch (GAW) regional stations
117 (<http://www.wmo.int/pages/prog/arep/gaw/measurements.html>). It is located on the northwest edge
118 of the Po Valley region, 60 km northwest of the Milan urban area. It can be regarded as a “regional/rural
119 background” site following the criteria recommended by the European Environment Agency (Larsen et
120 al., 1999). For simplicity, the term “regional background site” will be used in the following although
121 comparisons with rural background sites from other studies will also be reported. Further information
122 on the study site can be found in Putaud et al. (2014b).

123

124 2.2. Aerosol Chemical Speciation Monitor (ACSM)

125 The recently developed ACSM (Aerodyne Research Inc., ARI) was used to measure the non-refractory
126 (NR) chemical composition (organics, nitrate, sulfate, ammonium, chloride) of submicron particles (PM₁)
127 with a 30-min time resolution. The operating principle of the ACSM is similar to the widespread

128 Aerodyne aerosol mass spectrometer (Canagaratna et al., 2007; Jayne et al., 2000), with the difference
129 that the former does not inform on the size distribution of the chemical composition of NR-PM₁. A full
130 description of the ACSM can be found in Ng et al. (2011a). Briefly, an aerodynamic lens is used to focus
131 submicron particles (50% transmission range of 75-650 nm; Liu et al., 2007), which are then vaporized in
132 high vacuum, ionized by electron ionization (at 70 eV) and detected by a quadrupole mass spectrometer
133 (Pfeiffer Vacuum Prisma Plus RGA). Two different quadrupole-ACSMs (Q-ACSMs) were used in this study
134 (from March 2013 to February 2014): Q-ACSM#1 from 01 March to 18 August 2013 and Q-ACSM#2 from
135 20 June 2013 to 28 February 2014. Note that Q-ACSM#2 was not running from 3 November to 18
136 December due to its participation in the first inter-ACSM comparison exercise (Crenn et al., 2015). The
137 reproducibility and consistency with independent measurements are discussed in Sect. 3.1. In the
138 following, orthogonal regressions are reported unless otherwise stated.

139 Both ACSMs were operated with the latest Data Acquisition (DAQ 1.4.3.8 to 1.4.4.5) and Data
140 Analysis (DAS 1.5.3.0 to 1.5.3.2) software (ARI, <https://sites.google.com/site/ariacsm/mytemplate-sw>)
141 available at the time of use, which are developed within Igor Pro 6.32A (Wavemetrics).
142 Recommendations provided by Aerodyne (2010a, 2010b) and Ng et al. (2011a) were followed for the
143 operation, calibration and data analysis of the ACSMs. Ammonium nitrate calibrations were performed
144 seasonally and used for the determination of experimental nitrate response factors (RF) and ammonium
145 relative ionization efficiencies (RIE, see Sect. S1 for further details). Annual average and season-
146 dependent experimental RF and RIE values were alternatively applied to assess whether the ACSM is
147 stable over multi-seasonal periods (see Sect. 3.1 for results). Seasons are defined as spring (MAM),
148 summer (JJA), autumn (SON) and winter (DJF). RIEs for organics, nitrate and chloride (1.4, 1.1 and 1.3,
149 respectively) were taken from the literature (Canagaratna et al., 2007; Takegawa et al., 2005). RIE for
150 sulfate was experimentally determined based on ammonium sulfate calibrations for ACSM#2, and was
151 taken from the literature for ACSM#1 (see Sect. S1). Collection efficiencies (CE) set as i) a fixed 0.5 value
152 (e.g. Budisulistiorini et al., 2013) or ii) following the composition-dependent CE algorithm introduced by
153 Middlebrook et al. (2012) were compared in order to determine the most appropriate CEs (see Sect. 3.1
154 for results).

155

156 2.3. Additional analytical techniques

157 Additional measurements routinely performed at the JRC-Ispra site are used in this study (see Putaud et
158 al., 2014a for a full description). PM_{2.5} was sampled on quartz fibre filters (Pall, 2500 QAT-UP) with a
159 Partisol PLUS 2025 sampler equipped with a carbon honeycomb denuder operating at 16.7 L/min from

160 01 March 2013 to 28 February 2014 with daily filter changes at 08:00 UTC. Major ions (NH_4^+ , K^+ , NO_3^- ,
161 SO_4^{2-} , etc.) are analysed by ion chromatography (Dionex DX 120 with electrochemical eluent
162 suppression) after extraction in Milli-Q water (Millipore). Organic and elemental carbon (OC and EC,
163 respectively) are quantified by a thermal-optical method (Sunset Dual-optical Lab Thermal-Optical
164 Carbon Aerosol Analyzer) using the EUSAAR-2 protocol (Cavalli et al., 2010). Equivalent black carbon (BC)
165 is measured by a Multi Angle Absorption Photometer (MAAP, Thermo Scientific, model 5012) applying
166 an absorption cross section of $6.6 \text{ m}^2/\text{g}$ of equivalent black carbon at the operation wavelength of 670
167 nm. Particle volume concentrations are determined with a home-made Differential Mobility Particle
168 Sizer (DMPS) combining a Vienna-type Differential Mobility Analyser (DMA) and a Condensation Particle
169 Counter (CPC, TSI 3010), following the European Supersites for Atmospheric Aerosol Research (EUSAAR)
170 specifications for DMPS systems (Wiedensohler et al., 2012). Meteorological variables (temperature,
171 pressure, relative humidity, precipitation, wind speed and direction) are determined from a weather
172 transmitter WXT510 (Vaisala, Finland). Solar radiation is measured by a CM11 pyranometer (Kipp and
173 Zonen, The Netherlands).

174

175 2.4. Apportionment of the organic fraction

176 The organic fraction was apportioned using the Positive Matrix Factorization approach (PMF, Lanz et al.,
177 2007; Paatero and Tapper, 1994; Ulbrich et al., 2009; Zhang et al., 2011) by applying the Multilinear
178 Engine 2 algorithm (ME-2, Paatero, 2000) implemented in the SoFi tool (v4.8, Canonaco et al., 2013;
179 Crippa et al., 2014). Details on the theory and application of PMF and ME-2 can be found in the
180 aforementioned studies. Briefly, PMF aims at factorizing an initial X matrix (representing the temporal
181 variation of m/z signals here) into two F and G matrices (representing factor profiles and contributions,
182 respectively) putting a constraint of non-negativity on F and G matrices. Contrary to the classical
183 program used to resolve PMF (e.g. PMF2, PMF3), ME-2 allows any element of the F and G matrices to be
184 constrained with a certain degree of freedom. This ME-2 approach has been typically used to constrain
185 full factor profiles (e.g. Amato et al., 2009; Crippa et al., 2014), specific elemental ratios (e.g. Sturtz et
186 al., 2014) or specific species contribution (e.g. Crawford et al., 2005) in a given factor profile.

187 In our study, ME-2 is applied with and without constraining factor profiles (FPs), using the so-
188 called α -value approach (Canonaco et al., 2013) in the former case, which can be described as follows:

$$189 (f_{k,j})_{\text{solution}} = (f_{k,j})_{\text{reference}} \pm \alpha \cdot (f_{k,j})_{\text{reference}} \quad (1)$$

190 where k and j are the indexes for the factors and the species, respectively, $f_{k,j}$ is the element (k, j) of the
191 F matrix, the index “solution” stands for the PMF user solution, “reference” for the reference profile and

192 “ α ” is a scalar defined between 0 and 1 (e.g. applying an α -value of 0.10 lets $\pm 10\%$ variability to our FP
193 solution with respect to the reference FP). Following Crippa et al. (2014), we perform a sequence of runs
194 with i) unconstrained PMF, ii) fixed HOA, iii) fixed HOA and BBOA, iv) fixed HOA, BBOA and cooking OA
195 (COA) factors before selecting the most appropriate solution. Uncertainties are calculated using the DAS
196 1.5.3.0 version following the methodologies of Allan et al., 2003a and Ulbrich et al. (2009). m/z 12 and
197 13 are removed for SA analysis since negative signals are observed most of the time. Reference factor
198 profiles (RFPs) are taken from ambient deconvolved spectra from the Aerosol Mass Spectrometry (AMS)
199 spectral database (Ulbrich et al., 2015). HOA and BBOA profiles are taken from Ng et al. (2011c) (average
200 of profiles from multiple studies) and COA from Crippa et al. (2013). Different α -values are tested (see
201 Sect. 3.2) applying i) relative standard deviations of averaged RFPs defined for every m/z (i.e. assuming
202 that the chosen averaged RFPs are representative of our data set), ii) recommendations of Crippa et al.
203 (2014) based on the SA of 25 European AMS data sets and iii) comparison with independent
204 measurements (e.g. NO_x, CO, BC, etc.). Solutions from 2 to 8 factors are investigated in order to choose
205 the appropriate number of factors (see Sect. S2 and 3.2).

206

207 3. Quality assurance / quality control

208 3.1. Quality assurance / quality control of ACSM measurements

209 Ammonium nitrate calibrations performed on each ACSM are shown in Fig. S2. RF_{NO_3} and RIE_{NH_4} do not
210 present significant seasonal variability - e.g. for ACSM#2 $RF_{NO_3}=4.7E-11\pm 0.2E-11$ A. $\mu g^{-1}.m^3$ - , suggesting
211 constant calibration factors may be used throughout the campaign. On the other hand, calibration
212 factors exhibit substantial discrepancies between both ACSMs (e.g. RF_{NO_3} of $2.5E-11$ and $4.7E-11$ A. $\mu g^{-1}.m^3$
213 for ACSM#1 and #2, respectively), suggesting that instrument-specific factors are necessary.
214 Applying constant and composition-dependent CEs does not lead to noticeable differences (e.g. for NR-
215 PM_{10} : $r^2=0.97$, slope= 1.00 ± 0.00 , y-intercept= 0.10 ± 0.03 $\mu g/m^3$, $n=14842$) due to i) low sampling line RH
216 (e.g. typically below 30% for ACSM#2), and ii) few high-nitrate-content events (only 5% of data exhibits
217 ammonium nitrate mass fractions $>40\%$, defined as high by Middlebrook et al., 2012). The Middlebrook
218 et al. (2012) algorithm is however preferred since slightly acidic aerosols are observed at the study site
219 (on average sulfate plus nitrate against ammonium in $\mu eq/m^3$: $r^2=0.96$, slope= 1.21 ± 0.00 ,
220 intercept= 0.01 ± 0.00 $\mu eq/m^3$, $n=14842$).

221 A comparison performed between the two ACSMs used in this study during a 2-month summer
222 period is shown in Fig. S3. Very good correlations are observed for every chemical component
223 ($0.91 < r^2 < 0.98$, $n=1402$, hourly average) - chloride excluded - with slopes relatively close to one

224 (0.87<slopes<1.42), indicating a fairly good comparability between both instruments. One of the two
225 ACSMs also participated in the first-ever inter-ACSM comparison exercise performed between 13
226 different European Q-ACSMs during 3 weeks in Paris, France (Crenn et al., 2015). Satisfactory
227 performances - defined by $|z\text{-scores}|<2$ - are reported for our instrument regarding every chemical
228 component and NR-PM₁ mass, attesting the consistency of our measurements with other European
229 sites.

230 Measurements performed by the ACSM and independent off-line and on-line analytical
231 techniques are compared in Figure 1 and Table 1. An overall good agreement is found for every major
232 components throughout the year (typically $r^2>0.8$), although discrepancies are observable for specific
233 species and seasons. On the annual scale, a good agreement ($r^2=0.77$, $n=317$) is found between organics
234 from ACSM and OC from filter measurements in spite of expected filter sampling artefacts (Maimone et
235 al., 2011; Turpin et al., 2000; Watson et al., 2009). Even better agreements are observed on a seasonal
236 basis ($r^2\sim 0.9$), with steeper slopes in summer compared with winter, which likely reflects the different
237 degrees of oxygenation of organics among seasons (leading to different OM-to-OC ratios). However,
238 these slopes cannot be directly regarded as the OM-to-OC ratios due to i) differences in size fractions
239 between both methods (PM₁ for ACSM and PM_{2.5} for filter measurements) and ii) uncertainties related
240 to RIE_{Org} for ACSM measurements (Budisulistiorini et al., 2014; Ripoll et al., 2015). An estimation of the
241 OM-to-OC ratio for submicron organics applying the methodology described by Canagaratna et al.
242 (2015) is discussed in Sect. 4.2. Good correlations are observed for nitrate during all seasons ($r^2>0.9$) but
243 summer ($r^2=0.5$), which is most likely related to enhanced evaporative losses of ammonium nitrate from
244 filter during the latter season (Chow et al., 2005; Schaap et al., 2004). Slopes range from 0.9 to 1.4 -
245 summer excluded - which is comparable to what is reported elsewhere (Budisulistiorini et al., 2014;
246 Crenn et al., 2015; Ripoll et al., 2015). Very good correlations are observed for sulfate in every season
247 ($r^2=0.9-1.0$) with slopes close to 1 (0.9-1.1, winter excluded), consistent with its presence in the
248 submicronic size fraction and its low volatility leading to the minimization of sampling artefacts. Note
249 that discrepancies have been reported when comparing sulfate measured by the ACSM (Petit et al.,
250 2015) or the AMS (Zhang, 2005) with independent measurements. Our results suggest that ammonium
251 sulfate calibrations should be performed to experimentally determine sulfate RIEs, which appear to be
252 instrument-specific but stable over several months. Although aerosols are slightly acidic on average at
253 the study site, ammonium mostly neutralizes nitrate and sulfate throughout the campaign and thus
254 exhibits behaviour in between the two latter compounds. Higher uncertainties are associated with
255 chloride from filter quantification, resulting in no agreement with ACSM measurements in summer

256 when the concentrations are the lowest ($r^2=0.00$), and fairly good agreement during the other seasons
257 ($r^2=0.64-0.77$). The high slope observed for the ACSM#1 (e.g. 2.1 during spring) compared to the fairly
258 good slopes observed for ACSM#2 (0.7-1.1) suggests that chloride RIE might be instrument-specific and
259 require appropriate calibrations for its accurate quantification (see also Riffault et al., 2013 on this
260 topic).

261 The sum of NR-PM₁ components and BC has been compared to the volume concentration of
262 PM₁. Good agreement is found between both variables ($r^2>0.8$) giving further confidence on the
263 consistency of our ACSM measurements. The annual average particle density estimated from this
264 comparison (i.e. slope) is 1.6, which is typical of ambient aerosol particles densities (1.5-1.9 in Hand and
265 Kreidenweis, 2002; Hu et al., 2012; McMurry et al., 2002; Pitz et al., 2003, 2008). The higher densities
266 observed during spring and summer (1.9-2.0) than autumn and winter (1.3-1.5) are likely due to the
267 enhanced contribution of secondary aerosol and aged particles during the former period (Pitz et al.,
268 2008).

269

270 3.2. Quality assurance / quality control of organic source apportionment

271 First, during the aforementioned inter-ACSM comparison study (Crenn et al., 2015), source
272 apportionment of organics was performed based on data from 13 Q-ACSMs (Fröhlich et al., 2015),
273 including one ACSM used in the present study. Satisfactory performances ($|z\text{-scores}|<2$) are reported for
274 our ACSM using a similar approach as adopted in this study. This result demonstrates that our
275 instrument and the associated data treatment, including the source apportionment modelling, are
276 capable of accurately identifying and quantifying OA sources.

277

278 3.2.1. Model configurations

279 Regarding our specific study, the configuration applied to reach the optimal SA of organics is
280 thoroughly discussed in Sect. S2 (constrained factor profiles, number of factors, α -values and
281 integration-period durations). Briefly, constraining both HOA and BBOA factors result in satisfactory
282 solutions with relevant factor profiles, time series and daily cycles. Other configurations (e.g.
283 unconstrained factors) lead to unsatisfactory results with high seed variability, mixing of factors or
284 absence of key fragments in identified profiles (e.g. absence of m/z 43 and 44 in BBOA contrary to what
285 is reported in Heringa et al., 2011, Fig. S4). Solutions applying different number of factors are
286 investigated. Three-factors (HOA, BBOA and OOA) are retained during spring, autumn and winter
287 whereas two factors (HOA and OOA) are most suitable during summer. A lower number of factors

288 results in a mixing of them, whereas a higher number generates additional factors - e.g. semi-volatile
289 OOA (SV-OOA) during summer, OOA-BBOA during autumn - which are not satisfactory - e.g. missing
290 fragments or poor correlations with external data, see Table S1. BBOA cannot be clearly identified
291 during summer i.e. in this season agricultural waste burning contributions are estimated to be minor
292 (maximum 3-4% of OA, Sect. S2). Note that COA could not be evidenced, likely due to the type of site
293 studied (regional background) and the lower sensitivity, time- and mass-to-charge-resolution of the
294 ACSM compared to classical AMS instruments (further discussed in Sect. S2; see also Dall'Osto et al.,
295 2015 on this subject). Uncertainties associated with factor contributions are estimated by performing
296 sensitivity tests on α -values, which are regarded as the most subjective input parameters. Five scenarios
297 putting very low to very high constraints on the reference factor profiles have been defined (see Table
298 S2). Comparable solutions in terms of relative contributions (Fig. S5) and agreement with independent
299 measurements (Table S2) are found when applying low to high constraints following the empiric
300 recommendations of Crippa et al. (2014). Unsatisfactory solutions are generally reached under the
301 extreme scenarios (fully fixed factor profiles and m/z specific standard deviations of reference factor
302 profiles). We decided to apply low constraints (i.e. α -values of 0.1 and 0.5 for HOA and BBOA,
303 respectively) to let as much freedom as possible to our factor profiles while remaining in the range of
304 plausible solutions. SA was performed on 3-months, 6-months and 1-year datasets. Although
305 comparable solutions are found for each configuration (number of factors, factor profiles, diurnal cycles,
306 comparisons with external data), applying SA on seasonal datasets was preferred since i) the seasonal
307 variability of factor profiles is captured and ii) questionable results are observed in summer for 6-
308 months and 1-year configurations (see Sect. S2). When comparing the sum of OA factor concentrations
309 and measured OA on the annual scale, OA is very well modelled ($r^2=0.97$, slope= 0.98 ± 0.00 ,
310 intercept= $0.1\pm 0.0 \mu\text{g}/\text{m}^3$, $n=14842$).

311

312 3.2.2. Model optimal solution

313 Factor profiles, contributions and daily cycles of the optimal SA solution are presented in Figure
314 2. Independent factor profiles and time series are found for each season, which is a prerequisite for
315 having reliable SA solutions. HOA is identified during every season and exhibits a profile dominated by
316 alkyl fragments such as m/z 55 (from the $\text{C}_n\text{H}_{2n-1}^+$ ion series) and m/z 57 (from $\text{C}_n\text{H}_{2n+1}^+$ ion series; Ng et
317 al., 2011c). Its relative contribution is characteristic of traffic emissions, exhibiting a peak in the morning,
318 and higher contributions during weekdays than weekends (e.g. averages of 14 and 9%, respectively, in
319 autumn, Fig. S6). BBOA is found during every season except summer and has a profile similar to that of

320 HOA, except for the high contribution of m/z 60 ($C_2H_4O_2^+$) and 73 ($C_3H_5O_2^+$), which have been suggested
321 as biomass burning markers (Lee et al., 2010 and references therein). A distinct daily cycle with higher
322 contributions during night-time than daytime is observed, in addition to higher contributions during
323 weekends than weekdays (e.g. averages of 24 and 21%, respectively, in spring, Fig. S6), consistent with
324 residential heating emissions. The low BBOA concentrations modelled during late spring and early
325 autumn, as well as the small increased contribution observed during the morning also suggest
326 residential heating emissions. OOA is identified thanks to the predominant contribution of m/z 44 (CO_2^+)
327 and 43 ($C_2H_3O^+$). The higher contribution of f_{44} (defined as m/z 44 to total organic signal; 0.17-0.23
328 depending on seasons) with respect to f_{43} (defined similarly; 0.05-0.09) suggests that this OOA factor is
329 highly oxidized and presents low volatility (LV-) rather than semi-volatility (SV-) OOA characteristics (see
330 Jimenez et al., 2009 and Zhang et al., 2011 for definitions of these components). This statement is
331 supported by very good correlations ($r^2=0.96-0.99$) found between our unconstrained OOA profiles and
332 the average low-volatility OOA (LV-OOA) profile reported by Ng et al. (2011c) from 6 AMS studies.
333 Interestingly, our OOA profiles present slight seasonal differences that likely reflect changes in source
334 contributions and/or physical-chemical processes in this factor. For instance, f_{60} in OOA profiles is
335 enhanced in winter (0.014) compared with other seasons (0.001-0.004), which suggests that biomass
336 burning contributes to this factor during the aforementioned season, consistent with different studies
337 reporting f_{60} in secondary OA from biomass burning (e.g. Cubison et al., 2011; Heringa et al., 2011; see
338 Sect. S2). Note that the mass spectral resemblance of primary humic-like substances to LV-OOA might
339 also partly explain this observation (e.g. Young et al., 2015), i.e. that a small fraction of primary OA is
340 found in this factor. Daily cycles are comparable for all seasons with a bimodal pattern characterized by
341 a small peak during night-time and a prominent peak during daytime. The latter peak suggests that a
342 fraction of (LV-) OOA could be locally rather than regionally produced on the time scale of few hours
343 only, likely due to enhanced photochemical activities during daytime. The former peak could be due to i)
344 the condensation of highly oxygenated semi-volatile material favoured by night-time thermodynamic
345 conditions or ii) a contribution of SV-OOA in our OOA factor, which is generally dominated by LV-OOA.
346 The absence of an f_{44} night-time peak (Sect. 4.2) suggests that the second assumption is more probable
347 implying that both SV-OOA and LV-OOA influence our OOA factor.

348

349 3.2.3. Time series comparisons

350 Comparisons between our OA factors, m/z tracer and independent species time series are
351 shown in Table 2. OOA time series show very good agreement with Org_43 (organic signal at m/z 43)

352 and Org_44 ($r^2 > 0.8$ and 0.9 , respectively) and relatively good agreement with secondary inorganic
353 species (e.g. $r^2 \geq 0.5$ for ammonium), indicating that this factor can be regarded as a surrogate for
354 secondary organic aerosols. Comparisons with sulfate (a low-volatility species) and nitrate (a semi-
355 volatile species) confirm that our OOA factor might be a mix of SV- and LV-OOA, since better agreement
356 is found with one or the other compound depending on the season studied. BBOA exhibits very good
357 coefficients of determination when compared with its presumable fragment tracers Org_60 and Org_73
358 ($r^2 > 0.97$), giving further confidence on its appropriate quantification. Good correlations are generally
359 found between BBOA and BC ($r^2 \geq 0.5$, except for summer) indicating that a large proportion of BC stems
360 from biomass burning, consistent with previous findings at the study site (Gilardoni et al., 2011, from EC
361 measurements). A good agreement is also observed with CO ($r^2 \geq 0.7$), as already reported in the Alpine
362 valleys (e.g. Gaeggeler et al., 2008). HOA is not as well correlated with external data or specific m/z ,
363 which could be related to i) the absence of clear m/z tracers for this factor due to similarities with BBOA
364 profile, ii) the absence of clear external tracers due to co-emissions by fossil fuel and biomass burning
365 activities of BC, CO and NO_x and iii) possible uncertainties associated with the apportionment between
366 HOA and BBOA. The first two assumptions are supported by the better agreement observed between
367 HOA and m/z fragments or independent data during summer (e.g. $r^2 = 0.52$, $n = 2208$ between HOA and
368 BC) and specific months (e.g. May, September), when biomass burning contributions are negligible.
369 Although uncertainties associated with the accurate apportionment of HOA and BBOA cannot be
370 excluded (e.g. due to rotational ambiguity), several factors evidence the robustness of the results and
371 indicate that a mixing of both factors is unlikely, since HOA and BBOA present i) independent factor time
372 series during all seasons ($r^2 = 0.1-0.2$), ii) distinct and relevant daily cycles and iii) no significant α -value
373 variability.

374

375 4. Results and discussion

376 The meteorological representativeness of this one-year measurement is assessed by comparing the
377 solar irradiation, precipitation, and temperature monthly averages to the ones measured during 1990-
378 2010 at the study site (Fig. S7). Comparable seasonal averages are generally found in our study and
379 during the bidecadal reference period. Nevertheless compared to 1990-2010, Spring 2013 was rainier,
380 Summer 2013 slightly warmer and sunnier, and Winter 2013-2014 rainier. Further information regarding
381 the representativeness of measurements performed at the study site during the year 2013 can be found
382 in Putaud et al. (2014a).

383

384 4.1. Chemical composition of NR-PM₁

385 An overview of the chemical composition of NR-PM₁ retrieved during this campaign is shown in Figure 3.
386 The annual averaged NR-PM₁ mass reported here (14.2 µg/m³) ranges amongst the highest NR-PM₁
387 levels (7th out of 41 sites) reported at rural and urban downwind sites in Europe (Crippa et al., 2014) and
388 worldwide (Jimenez et al., 2009; Zhang et al., 2007, 2011). Please note that these previous studies are
389 based on typically one month of measurements in different seasons. It is comparable to NR-PM₁ levels
390 reported during specific campaigns in the urban areas of New York City (USA, 12 µg/m³, Weimer et al.,
391 2006), Tokyo (Japan, 12-15 µg/m³, Takegawa et al., 2006) or Manchester (UK, 14 µg/m³, Allan et al.,
392 2003a, 2003b). Our annual average NR-PM₁ mass is higher than the 10 µg/m³ guideline given by the
393 World Health Organization for the annual average PM_{2.5} mass (including refractory and non-refractory
394 compounds; WHO, 2006). After similar conclusions have been drawn for PM_{2.5} and PM₁₀ size fractions
395 (Putaud et al., 2010), the Po Valley appears to be one of the most polluted regions in Europe with regard
396 to NR-PM₁ levels this time. Submicron aerosol particles are mostly made of organics (58%), nitrate
397 (21%), sulfate (12%) and ammonium (8%; Figure 3). The predominance of organics is typical of urban
398 downwind sites (e.g. average of 52% reported in Zhang et al., 2011). On the other hand, the noticeable
399 proportion of nitrate is characteristic of urban sites (18% in Zhang et al., 2011), which likely reflects the
400 substantial influence of anthropogenic activities emissions at our regional site. As a result, sulfate
401 exhibits particularly low contributions at the study site compared with other locations (generally >20%
402 in Zhang et al., 2011).

403 NR-PM₁ levels present a clear seasonality with higher levels during spring (~18 µg/m³) and
404 winter (~15 µg/m³) compared with summer and autumn (~12 µg/m³). Higher levels were expected
405 during cold months due to enhanced biomass burning emissions and lower boundary layer heights
406 (BLH), as previously observed at the study site (Putaud et al., 2013). Expected seasonal variations of the
407 chemical composition of NR-PM₁ are observed, with i) higher nitrate contributions during the cold
408 season which favours its partitioning in the condensed phase (Clegg et al., 1998), ii) higher sulfate
409 contributions during summer, which can e.g. be associated with enhanced photochemical production
410 (Seinfeld and Pandis, 2006) and lower amount of rainout (Fig. S7), and iii) relatively stable contributions
411 for ammonium (mainly neutralizing the two previous species) and organics (discussed later on).

412 A focus will now be made on daily cycles of the chemical composition of NR-PM₁ (Figure 4),
413 displayed for the first time during the 4 seasons in the Po Valley, thanks to the high time resolution and
414 stability of the ACSM. On the annual scale, daily cycles of NR-PM₁ levels are characterized by
415 significantly higher concentrations during night-time than daytime, likely due to lower BLH, higher wood

416 burning emissions (during cold seasons) and lower temperatures favouring the partitioning of semi-
417 volatile inorganic (mainly ammonium nitrate) and organic material in the condensed phase, to name a
418 few. A distinct peak is however observed around noon, probably caused by enhanced photochemical
419 production of secondary organic compounds, and increased BLH favouring downward mixing of
420 advected pollution, especially during summer (Figure 4; Decesari et al., 2014). Note that this annual daily
421 pattern is the combination of distinct daily cycles varying with the season studied (Figure 4). In terms of
422 relative chemical composition, organics are dominating NR-PM₁ mass independently of the time of the
423 day, with median contributions ranging from ~60 to 70%. Nitrate exhibits higher contribution during
424 night-time due to its abovementioned semi-volatile nature. Sulfate shows unexpected daily cycles with
425 significantly different (99.99% confidence level) relative contributions - and absolute concentrations -
426 during daytime (~15% of NR-PM₁ mass around noon) compared to night-time (~10% around midnight,
427 Figure 4), although its formation was expected to occur mainly over longer time scales (i.e. days) in
428 cloud droplets (Ervens et al., 2011). This observation could be due to i) local production of sulfate with
429 increased photochemical production around noon at the study site and/or ii) diurnal changes of the
430 atmospheric stratification in the Po Valley as described by Saarikoski et al. (2012) and Decesari et al.
431 (2014), enhancing aged particle contribution during the middle of the day and the afternoon. Non-
432 refractory chloride (mostly NH₄Cl, Huang et al., 2010) exhibits very low contributions independently of
433 the hour of the day (medians below 0.5% of NR-PM₁ mass) with however a slight increase at night,
434 which is likely due to its presumable semi-volatile nature here.

435

436 4.2. Focus on organic aerosols

437 An overview of the contribution of HOA, BBOA and OOA to OA is shown in Figure 5. On the annual
438 average, the organic fraction is dominated by the secondary component (OOA, 66%). Although this OOA
439 contribution is substantial, higher proportions are generally reported at rural and urban downwind sites
440 worldwide (90 and 82% of OA on average, respectively, Zhang et al., 2011). This lower relative
441 contribution of OOA is related to the higher contribution of (primary) BBOA in our study (23% of OA on
442 the annual average) compared to the previous ones. Considerable contributions of BBOA are explained
443 by the specific location of the study site in the vicinity of the Alps, where biomass burning is a major
444 contributor to OA (Belis et al., 2011; Herich et al., 2014; Lanz et al., 2010). Biomass burning emissions
445 hence substantially affect OA levels on the annual scale here. The contribution of HOA is comparatively
446 smaller (11%), indicating that despite the expected large contributions of fossil fuel emissions (i.e. traffic
447 and industrial emissions), those are not the major sources of primary OA at the study site. On the other

448 hand, it is likely that fossil fuel emissions of volatile organic compounds (VOCs) - which are OOA
449 precursors - contribute to our OOA levels as reported elsewhere (Gentner et al., 2012; Volkamer et al.,
450 2006). At the study site, Gilardoni et al. (2011) previously estimated on the basis of ^{14}C analyses that
451 secondary organic carbon stemming from fossil emissions might represent 12% of OC on the annual
452 average. In other words, fossil fuel emissions could represent approximately a quarter (12+11=23%) of
453 total OA mass when both primary and secondary OA fractions are accounted for. The analysis of the
454 components' seasonal variations shows relatively stable HOA contributions (9-14%), higher
455 contributions of BBOA during cold seasons due to residential heating (up to 36% of OA on average
456 during winter) and higher OOA contributions during summer related to enhanced photochemical
457 production (86% of OA on average).

458 OA can be further characterized investigating specific organic fragments. m/z 44 (mainly CO_2^+)
459 and 43 (mainly $\text{C}_2\text{H}_3\text{O}^+$) signals give insights on the nature of OA, as the former is primarily related to
460 acids or acid-derived species whereas the latter is mostly associated with non-acid oxygenates (Duplissy
461 et al., 2011; Ng et al., 2011b). Daily variations of both f_{44} and f_{43} are shown in Figure 6, along with other
462 major organic fragments. On average, f_{44} is predominant with respect to f_{43} (15 and 7%, respectively),
463 which indicates that acid species dominate the OA composition with respect to non-acid oxygenates.
464 Both fragments present different daily patterns underlying distinct mechanisms of formation. Acids'
465 contributions are enhanced during daytime, which could be explained by photochemical processes
466 and/or daily BLH variations as already discussed for sulfate. Non-acid oxygenates exhibit higher
467 contributions during night-time than daytime. This pattern could be due to i) the formation of semi-
468 volatile non-acids during night-time by e.g. condensation (Lanz et al., 2007), ii) their degradation during
469 daytime by e.g. fragmentation reactions (Daumit et al., 2013) and/or iii) their conversion into acid-
470 related species during daytime by e.g. functionalization or oligomerization reactions (Daumit et al.,
471 2013). It should be specified that the enhancement of f_{44} during daytime and the increasing of f_{43} during
472 night-time only represent a small fraction of their total contributions to OA (Figure 6), suggesting that
473 most acid and non-acid oxygenates have been formed before reaching our sampling site, i.e. have been
474 imported from other regions. The other major OA fragments (m/z 29, 55, 57 and 60) present i) constant
475 contributions for f_{29} due its various emission sources (HOA, BBOA, OOA; Ng et al., 2011c), ii) the absence
476 of lunch peak for f_{55} (and also for the absolute contributions of m/z 55) consistent with the presumable
477 low influence of cooking emissions, iii) morning and evening peaks for f_{57} characteristic of fossil fuel
478 emissions and iv) higher contributions during night-time for f_{60} in agreement with its biomass burning
479 origin.

480 Using f_{43} and f_{44} , the oxygen-to-carbon (O/C), OM-to-OC (OM/OC), hydrogen-to-carbon (H/C)
481 ratios and the carbon oxidation state (OSc) have been estimated for total OA based on the
482 methodologies described by Aiken et al. (2008), Kroll et al. (2011) and Ng et al. (2011b), and applying the
483 parameterization defined in Canagaratna et al. (2015), which can be summarized as follows:

$$484 \text{ O/C} = 4.31 f_{44} + 0.079 \quad (1)$$

$$485 \text{ OM/OC} = 1.28 \text{ O/C} + 1.17 \quad (2)$$

$$486 \text{ H/C} = 1.12 + 6.74 f_{43} - 17.77 f_{43}^2 \quad (3)$$

$$487 \text{ OSc} = 2 * \text{O/C} - \text{H/C} \quad (4)$$

488 with H/C (and therefore OSc) being estimated only if $f_{44} > 0.05$ and $f_{43} > 0.04$ (Canagaratna et al., 2015).
489 Uncertainties associated with these estimates - in particular based on ACSM measurements - are
490 discussed in Sect. S3 (see also Fig. S8). Comparisons with studies using (HR-ToF-) AMS instruments will
491 not be reported and only variations within this dataset will be discussed (see Sect. S3). Seasonal and
492 annual O/C, OM/OC, H/C and OSc are shown in Figure 7. High O/C, OM/OC and OSc are found on the
493 annual scale (medians of 0.7, 2.1 and -0.2, respectively), reflecting once more the aged, oxidized
494 properties of organic matter at the study site, consistent with the predominance of the OOA
495 component. Little seasonal variations are observed for the aforementioned variables hence highlighting
496 the high degree of oxidation of OA throughout the year (Figure 7). The unexpectedly high degree of
497 oxygenation of OA observed during cold seasons despite the increased contribution of primary BBOA
498 (with OM/OC ratios of 1.4-1.6) could be explained by the contribution of secondary BBOA in our OOA
499 factor during these cold seasons, which could be associated with the enhancement of e.g. dicarboxylic
500 and ketocarboxylic acid contents (Kundu et al., 2010) that have extremely high OM/OC ratios (up to 3.8
501 and 3.1, respectively, Turpin and Lim, 2001). This assumption is supported by the higher proportion of
502 f_{60} in our OOA factor (discussed in Sect. 3.2 and S2), as well as the surprisingly high OM/OC ratio
503 observed for OOA during winter (2.5 compared to 2.2-2.4 during the other seasons). Note that
504 Canonaco et al. (2015) also report a higher f_{44} in (LV-) OOA in winter compared to summer in Zurich
505 (Switzerland). According to these authors, this could be due to enhanced aqueous-phase production of
506 (LV-) OOA in clouds or hygroscopic aerosols in winter, which would lead to higher levels of oxygenation
507 compared to gas-phase oxidation mechanisms typically occurring during summer.

508

509 4.3. Possible implications for PM abatement strategies

510 In order to investigate the characteristics of fine aerosol pollution events, the variations of NR-PM₁
511 chemical composition and OA factors' contributions as a function of total NR-PM₁ mass are examined.

512 This investigation is made on the annual (Figure 8, discussion below) and seasonal scales (Fig. S9,
513 discussion in Sect. S4). Distinct trends are observed depending on the chemical species and OA
514 components studied. The proportion of nitrate is clearly enhanced with increasing NR-PM₁ levels (from
515 ~10 to >30% when [NR-PM₁] > 30 µg/m³) indicating that nitrate - or NO_x - abatement policies should be
516 highly effective when attempting to limit PM₁ pollution events in the Upper Po Valley. Sulfate shows an
517 opposite trend with decreasing relative contribution when NR-PM₁ mass increases (e.g. <5% when [NR-
518 PM₁] > 50 µg/m³), likely due to the lower concentrations of sulfate during cold seasons, when the highest
519 number of pollution events is observed. The proportion of organics is substantial (48-66%)
520 independently of NR-PM₁ mass, justifying once again the importance of determining its sources to
521 design adequate abatement policies. When focusing on the organic fraction, BBOA is the only OA factor
522 exhibiting increased contributions (from ~10 to >40%) with increased NR-PM₁ mass (from <10 to >60
523 µg/m³), which points out the PM abatement potential of effective biomass burning emission reductions.
524 HOA levels are rather constant throughout the year and therefore their proportions steadily decrease
525 when NR-PM₁ levels increase, implying that local fossil fuel related emissions of primary OC are not the
526 main responsible for submicron pollution events observed at the study site on the annual scale.
527 Although OOA always represents a major fraction of OA (41-75% depending on the mass bin studied), its
528 contribution steadily decreases with increasing NR-PM₁ mass. This unexpected result signifies that even
529 though aged, secondary, oxidised organics are the main contributor to OA on the annual average (66%),
530 they do not play a prominent role in fine PM acute pollution events.

531 Current European legislations set daily and/or annual PM limit values depending on the size fraction
532 addressed (Directive 2008/50/EC). Volume size distributions suggest that approximately 90% of the
533 PM_{2.5} mass concentration is borne by particles below an aerodynamic diameter of 1 µm at the study site
534 (Putaud et al., 2014a). Therefore, measures tackling the main constituents of the submicron aerosol
535 fraction would be efficient for complying with PM_{2.5} legislations. Based on the chemical characterization
536 of NR-PM₁ and SA of its organic fraction with a time-resolution of 30 min over 1-year, this study provides
537 new evidence which could orient PM abatement strategies also at similar regional background sites of
538 the Po Valley. On the annual scale, OA and especially OOA should be of main concern given their
539 predominance in NR-PM₁ chemical composition (Figure 3). On the seasonal scale, efforts should be
540 directed towards the cold seasons (winter and early spring), for which the highest NR-PM₁ levels are
541 observed, due to specific meteorological conditions (e.g. low BLH, low temperatures) and emission
542 sources (e.g. biomass burning, Figure 3 and Figure 5). In particular, measures addressing emissions of

543 NO_x and BBOA would be the most efficient for reducing the magnitude and frequency of PM pollution
544 events (Figure 8).

545 Recommendations for PM abatement strategies are formulated here from a legislative perspective,
546 which aims at decreasing PM levels. Although diminishing PM levels should help reducing PM impacts,
547 the existence of a direct causal relationship can be debatable since each chemical component has a
548 specific effect on human health (WHO, 2013), the radiative forcing (Boucher et al., 2013) or ecosystems
549 (e.g. Carslaw et al., 2010). For instance, implementing policies aiming at mitigating nitrate
550 concentrations - as suggested previously in this section - would likely have limited health benefits
551 according to toxicological studies (Reiss et al., 2007; Schlesinger and Cassee, 2003), and should lead to
552 an increased global warming (Boucher et al., 2013). On the other hand, measures reducing BBOA levels
553 should be beneficial, since the cardio-vascular effects of biomass burning particles have been widely
554 reported in the literature (Bølling et al., 2009; Miljevic et al., 2010; Naeher et al., 2007) and could be
555 similar to those of traffic-emitted particles (WHO, 2013 and references therein), whereas their impacts
556 on the radiative forcing could be null (Boucher et al., 2013). Strategies aiming at reducing solely PM
557 mass are therefore limited, and an assessment of their impacts - e.g. using integrated assessment
558 models (Carnevale et al., 2012; Janssen et al., 2009) with appropriate parameterizations of fundamental
559 processes - would be beneficial.

560

561 5. Conclusion and perspectives

562 The NR-PM₁ chemical composition and the apportionment of the organic fraction have been
563 investigated for the first time with this completeness at a regional background site of the Po valley
564 (Italy), using high time-resolution (30 min) and long term (1 year) measurements with a state-of-the-art
565 quality assured ACSM and the most advanced factor analysis methods. Comparisons between two
566 ACSMs show very good time series correlations for the major compounds ($0.91 < r^2 < 0.98$, $n=1402$) with
567 however discrepancies in their absolute concentrations ($0.9 < \text{slopes} < 1.4$). These results are promising
568 with regard to the consistency of ACSM measurements at different locations, but also underlines the
569 importance of conducting inter-ACSM comparisons to define common protocols and assure data
570 comparability among the European ACSM network (see Crenn et al., 2015). Comparisons between ACSM
571 and independent analytical technique measurements show an overall good agreement for major
572 components throughout the year (typically $r^2 > 0.8$). Discrepancies observed in time series correlations
573 and quantifications (i.e. slopes) for specific species and seasons (e.g. nitrate in summer) are attributed
574 to filter sampling artefacts. These results are encouraging regarding the potential implementation of

575 ACSMs in air quality networks as a replacement of traditional filter-based techniques, to measure the
576 artefact-free chemical composition of fine aerosols with high time-resolution. Additional comparison
577 studies are nevertheless needed to support our results, and further technical development allowing the
578 refractory carbon fraction to be accounted for is required.

579 NR-PM₁ and PM₁ levels measured in the upper Po Valley (14.2 and 15.3 µg/m³ on the annual
580 average, respectively) are among the highest reported in Europe, stressing the need for implementing
581 effective PM abatement strategies in this region. On average, the chemical composition of non-
582 refractory submicron aerosol is dominated by organic aerosol (58% of NR-PM₁), which is composed of
583 HOA (11% of OA), BBOA (23%) and OOA (66%). Fossil fuel combustion is thus not a major source of
584 primary OA in this area of the Po Valley. Primary BBOA significantly contributes to OA on the annual
585 average and especially during winter (36%). Our OOA component is highly oxidised and aged with an LV-
586 OOA spectral signature, a large proportion of acid-related species and high OM/OC ratios. Highly
587 oxidised OA properties are observed during all seasons, surprisingly including winter, which could reflect
588 secondary BBOA influence and OOA aqueous-phase formation processes during cold seasons. Further
589 research aiming at identifying the sources of OOA - including secondary BBOA using e.g. high resolution
590 mass spectrometric techniques (Crippa et al., 2013) or proton nuclear magnetic resonance (Paglione et
591 al., 2014) - and better estimating O/C, OM/OC and OSc parameters would be beneficial.

592 Specific recommendations for PM abatement strategies at a regional level can be suggested.
593 The higher frequency of particulate pollution peaks observed during cold seasons suggests an
594 orientation of future policies towards these periods. BBOA and nitrate present increasing relative
595 contributions with increasing fine aerosol levels, which suggests that wood burning and NO_x emission
596 reductions should notably decrease NR-PM₁ pollution events. Note that these recommendations are
597 only formulated in the perspective of reducing PM levels, assuming a subsequent reduction of PM
598 impacts. Additional dimensions - e.g. specific impacts of each chemical component, short versus long-
599 term exposure, co-benefit of sanitary and climatic impacts - should also be considered when defining
600 PM abatement strategies. In a broader context, the use of high time resolution analytical techniques for
601 the measurement of PM pollution properties can help better shape our future air quality policies.

602
603 *Acknowledgements.* This study was partially supported by the European Union's project ACTRIS
604 (Aerosols, Clouds, and Trace gases Research InfraStructure Network, EU FP7-262254). R. Passarella (EC-
605 JRC), K. Douglas (EC-JRC), V. Pedroni (EC-JRC) and M. Stracquadanio (ENEA) are thanked for their help on
606 the field and/or for the chemical analyses of filters. P. Croteau (Aerodyne) is acknowledged for his

607 technical support on the operation of the ACSM. N. Jensen (EC-JRC) is thanked for providing gas phase
608 data. M. Crippa (EC-JRC) is acknowledged for her valuable advices.

609 **References**

610

- 611 Aerodyne: Aerosol Chemical Speciation Monitor: Data Acquisition Software Manual, available at:
612 ftp://ftp.aerodyne.com/ACSM/ACSM_Manuals/ACSM_DAQ_Manual.pdf (last access: 15
613 February 2016), 2010a.
- 614 Aerodyne: Aerosol Chemical Speciation Monitor: Data Analysis Software Manual, available at:
615 ftp://ftp.aerodyne.com/ACSM/ACSM_Manuals/ACSM_Igor_Manual.pdf (last access: 15
616 February 2016), 2010b.
- 617 Aiken, A. C., DeCarlo, P. F., Kroll, J. H., Worsnop, D. R., Huffman, J. A., Docherty, K. S., Ulbrich, I. M.,
618 Mohr, C., Kimmel, J. R., Sueper, D., Sun, Y., Zhang, Q., Trimborn, A., Northway, M., Ziemann, P.
619 J., Canagaratna, M. R., Onasch, T. B., Alfarra, M. R., Prevot, A. S. H., Dommen, J., Duplissy, J.,
620 Metzger, A., Baltensperger, U., and Jimenez, J. L.: O/C and OM/OC ratios of primary, secondary,
621 and ambient organic aerosols with high-resolution time-of-flight aerosol mass spectrometry,
622 *Environ. Sci. Technol.*, 42(12), 4478–4485, doi:10.1021/es703009q, 2008.
- 623 Allan, J. D., Jimenez, J. L., Williams, P. I., Alfarra, M. R., Bower, K. N., Jayne, J. T., Coe, H., and Worsnop,
624 D. R.: Quantitative sampling using an Aerodyne aerosol mass spectrometer 1. Techniques of
625 data interpretation and error analysis, *J. Geophys. Res.-Atmos.*, 108(D3), 4090,
626 doi:10.1029/2002JD002358, 2003a.
- 627 Allan, J. D., Alfarra, M. R., Bower, K. N., Williams, P. I., Gallagher, M. W., Jimenez, J. L., McDonald, A. G.,
628 Nemitz, E., Canagaratna, M. R., Jayne, J. T., Coe, H., and Worsnop, D. R.: Quantitative sampling
629 using an Aerodyne aerosol mass spectrometer 2. Measurements of fine particulate chemical
630 composition in two U.K. cities, *J. Geophys. Res.-Atmos.*, 108(D3), 4091,
631 doi:10.1029/2002JD002359, 2003b.
- 632 Amato, F., Pandolfi, M., Escrig, A., Querol, X., Alastuey, A., Pey, J., Perez, N., and Hopke, P. K.:
633 Quantifying road dust resuspension in urban environment by Multilinear Engine: a comparison
634 with PMF2, *Atmos. Environ.*, 43(17), 2770–2780, doi:10.1016/j.atmosenv.2009.02.039, 2009.
- 635 Belis, C. A., Cancelinha, J., Duane, M., Forcina, V., Pedroni, V., Passarella, R., Tanet, G., Douglas, K.,
636 Piazzalunga, A., Bolzacchini, E., Sangiorgi, G., Perrone, M.-G., Ferrero, L., Fermo, P., and Larsen,
637 B. R.: Sources for PM air pollution in the Po Plain, Italy: I. Critical comparison of methods for
638 estimating biomass burning contributions to benzo(a)pyrene, *Atmos. Environ.*, 45(39), 7266–
639 7275, doi:10.1016/j.atmosenv.2011.08.061, 2011.
- 640 Belis, C. A., Karagulian, F., Larsen, B. R., and Hopke, P. K.: Critical review and meta-analysis of ambient
641 particulate matter source apportionment using receptor models in Europe, *Atmos. Environ.*, 69,
642 94–108, doi:10.1016/j.atmosenv.2012.11.009, 2013.
- 643 Bølling, A. K., Pagels, J., Yttri, K., Barregard, L., Sallsten, G., Schwarze, P. E., and Boman, C.: Health effects
644 of residential wood smoke particles: the importance of combustion conditions and
645 physicochemical particle properties, *Part. Fibre Toxicol.*, 6(1), 29, doi:10.1186/1743-8977-6-29,
646 2009.
- 647 Boucher, O., Randall, D., Artaxo, P., Bretherton, C., Feingold, G., Forster, P., Kerminen, V.-M., Kondo, Y.,
648 Liao, H., Lohmann, U., Rasch, P., Satheesh, S. K., Sherwood, S., Stevens, B., and Zhang, X.: Clouds
649 and aerosols, in *Climate Change 2013: The Physical Science Basis. Contribution of Working
650 Group I to the Fifth Assessment Report of the Intergovernmental Panel on Climate Change*,
651 edited by: Stocker, T. F., Qin, D., Plattner, G.-K., Tignor, M., Allen, S. K., Boschung, J., Nauels,
652 A., Xia, Y., Bex, V., and Midgley, P. M., Cambridge University Press, Cambridge, United Kingdom
653 and New York, NY, USA, 2013.
- 654 Budisulistiorini, S. H., Canagaratna, M. R., Croteau, P. L., Marth, W. J., Baumann, K., Edgerton, E. S.,
655 Shaw, S. L., Knipping, E. M., Worsnop, D. R., Jayne, J. T., Gold, A., and Surratt, J. D.: Real-time

656 continuous characterization of secondary organic aerosol derived from isoprene epoxydiols in
657 downtown Atlanta, Georgia, using the Aerodyne aerosol chemical speciation monitor, *Environ.*
658 *Sci. Technol.*, 47(11), 5686–5694, doi:10.1021/es400023n, 2013.

659 Budisulistiorini, S. H., Canagaratna, M. R., Croteau, P. L., Baumann, K., Edgerton, E. S., Kollman, M. S., Ng,
660 N. L., Verma, V., Shaw, S. L., Knipping, E. M., Worsnop, D. R., Jayne, J. T., Weber, R. J., and
661 Surratt, J. D.: Intercomparison of an aerosol chemical speciation monitor (ACSM) with ambient
662 fine aerosol measurements in downtown Atlanta, Georgia, *Atmos. Meas. Tech.*, 7(7), 1929–
663 1941, doi:10.5194/amt-7-1929-2014, 2014.

664 Canagaratna, M. R., Jayne, J. T., Jimenez, J. L., Allan, J. D., Alfarra, M. R., Zhang, Q., Onasch, T. B.,
665 Drewnick, F., Coe, H., Middlebrook, A., Delia, A., Williams, L. R., Trimborn, A. M., Northway, M.
666 J., DeCarlo, P. F., Kolb, C. E., Davidovits, P., and Worsnop, D. R.: Chemical and microphysical
667 characterization of ambient aerosols with the Aerodyne aerosol mass spectrometer, *Mass*
668 *Spectrom. Rev.*, 26(2), 185–222, doi:10.1002/mas.20115, 2007.

669 Canagaratna, M. R., Jimenez, J. L., Kroll, J. H., Chen, Q., Kessler, S. H., Massoli, P., Hildebrandt Ruiz, L.,
670 Fortner, E., Williams, L. R., Wilson, K. R., Surratt, J. D., Donahue, N. M., Jayne, J. T., and Worsnop,
671 D. R.: Elemental ratio measurements of organic compounds using aerosol mass spectrometry:
672 characterization, improved calibration, and implications, *Atmos. Chem. Phys.*, 15, 253–272,
673 doi:10.5194/acp-15-253-2015, 2015.

674 Canonaco, F., Crippa, M., Slowik, J. G., Baltensperger, U., and Prévôt, A. S. H.: SoFi, an IGOR-based
675 interface for the efficient use of the generalized multilinear engine (ME-2) for the source
676 apportionment: ME-2 application to aerosol mass spectrometer data, *Atmos. Meas. Tech.*,
677 6(12), 3649–3661, doi:10.5194/amt-6-3649-2013, 2013.

678 Canonaco, F., Slowik, J. G., Baltensperger, U., and Prévôt, A. S. H.: Seasonal differences in oxygenated
679 organic aerosol composition: implications for emissions sources and factor analysis, *Atmos.*
680 *Chem. Phys.*, 15(12), 6993–7002, doi:10.5194/acp-15-6993-2015, 2015.

681 Carbone, C., Decesari, S., Paglione, M., Giulianelli, L., Rinaldi, M., Marinoni, A., Cristofanelli, P.,
682 Didiodato, A., Bonasoni, P., Fuzzi, S., and Facchini, M. C.: 3-year chemical composition of free
683 tropospheric PM₁ at the Mt. Cimone GAW global station – South Europe – 2165 m a.s.l., *Atmos.*
684 *Environ.*, 87, 218–227, doi:10.1016/j.atmosenv.2014.01.048, 2014.

685 Carnevale, C., Finzi, G., Pisoni, E., Volta, M., Guariso, G., Gianfreda, R., Maffei, G., Thunis, P., White, L.,
686 and Triacchini, G.: An integrated assessment tool to define effective air quality policies at
687 regional scale, *Environ. Modell. Softw.*, 38, 306–315, doi:10.1016/j.envsoft.2012.07.004, 2012.

688 Carslaw, K. S., Boucher, O., Spracklen, D. V., Mann, G. W., Rae, J. G. L., Woodward, S., and Kulmala, M.: A
689 review of natural aerosol interactions and feedbacks within the Earth system, *Atmos. Chem.*
690 *Phys.*, 10(4), 1701–1737, 2010.

691 Cavalli, F., Viana, M., Yttri, K. E., Genberg, J., and Putaud, J. P.: Toward a standardised thermal-optical
692 protocol for measuring atmospheric organic and elemental carbon: the EUSAAR protocol,
693 *Atmos. Meas. Tech.*, 3, 79–89, 2010.

694 Chow, J. C., Watson, J. G., Lowenthal, D. H., and Magliano, K. L.: Loss of PM_{2.5} nitrate from filter samples
695 in central California, *J. Air Waste Manage. Assoc.*, 55(8), 1158–1168,
696 doi:10.1080/10473289.2005.10464704, 2005.

697 Clegg, S. L., Brimblecombe, P., and Wexler, A. S.: Thermodynamic model of the system H⁺-NH₄⁺-SO₄²⁻
698 -NO₃⁻-H₂O at tropospheric temperatures, *J. Phys. Chem. A*, 102(12), 2137–2154,
699 doi:10.1021/jp973042r, 1998.

700 Clerici, M. and Mélin, F.: Aerosol direct radiative effect in the Po Valley region derived from AERONET
701 measurements, *Atmos. Chem. Phys.*, 8(16), 4925–4946, 2008.

702 Crawford, J., Cohen, D., Dyer, L., and Zahorowski, W.: Receptor modelling with PMF2 and ME2 using
703 aerosol data from Hong Kong, Australian Nuclear Science and Technology Organisation (ANSTO),

704 available at: <http://apo.ansto.gov.au/dspace/bitstream/10238/201/1/ANSTO-E-756.pdf> (last
705 access: 15 February 2016), 2005.

706 Crenn, V., Sciare, J., Croteau, P. L., Verlhac, S., Fröhlich, R., Belis, C. A., Aas, W., Äijälä, M., Alastuey, A.,
707 Artiñano, B., Baisnée, D., Bonnaire, N., Bressi, M., Canagaratna, M., Canonaco, F., Carbone, C.,
708 Cavalli, F., Coz, E., Cubison, M. J., Esser-Gietl, J. K., Green, D. C., Gros, V., Heikkinen, L.,
709 Herrmann, H., Lunder, C., Minguillón, M. C., Močnik, G., O’Dowd, C. D., Ovadnevaite, J., Petit, J.-
710 E., Petralia, E., Poulain, L., Priestman, M., Riffault, V., Ripoll, A., Sarda-Estève, R., Slowik, J. G.,
711 Setyan, A., Wiedensohler, A., Baltensperger, U., Prévôt, A. S. H., Jayne, J. T., and Favez, O.:
712 ACTRIS ACSM intercomparison – part 1: reproducibility of concentration and fragment results
713 from 13 individual quadrupole aerosol chemical speciation monitors (Q-ACSM) and consistency
714 with co-located instruments, *Atmos. Meas. Tech.*, 8(12), 5063–5087, doi:10.5194/amt-8-5063-
715 2015, 2015.

716 Crippa, M., DeCarlo, P. F., Slowik, J. G., Mohr, C., Heringa, M. F., Chirico, R., Poulain, L., Freutel, F., Sciare,
717 J., Cozic, J., Di Marco, C. F., Elsasser, M., Nicolas, J. B., Marchand, N., Abidi, E., Wiedensohler, A.,
718 Drewnick, F., Schneider, J., Borrmann, S., Nemitz, E., Zimmermann, R., Jaffrezo, J.-L., Prévôt, A. S.
719 H., and Baltensperger, U.: Wintertime aerosol chemical composition and source apportionment
720 of the organic fraction in the metropolitan area of Paris, *Atmos. Chem. Phys.*, 13(2), 961–981,
721 doi:10.5194/acp-13-961-2013, 2013.

722 Crippa, M., Canonaco, F., Lanz, V. A., Äijälä, M., Allan, J. D., Carbone, S., Capes, G., Ceburnis, D.,
723 Dall’Osto, M., Day, D. A., DeCarlo, P. F., Ehn, M., Eriksson, A., Freney, E., Hildebrandt Ruiz, L.,
724 Hillamo, R., Jimenez, J. L., Junninen, H., Kiendler-Scharr, A., Kortelainen, A.-M., Kulmala, M.,
725 Laaksonen, A., Mensah, A. A., Mohr, C., Nemitz, E., O’Dowd, C., Ovadnevaite, J., Pandis, S. N.,
726 Petäjä, T., Poulain, L., Saarikoski, S., Sellegri, K., Swietlicki, E., Tiitta, P., Worsnop, D. R.,
727 Baltensperger, U., and Prévôt, A. S. H.: Organic aerosol components derived from 25 AMS data
728 sets across Europe using a consistent ME-2 based source apportionment approach, *Atmos.*
729 *Chem. Phys.*, 14(12), 6159–6176, doi:10.5194/acp-14-6159-2014, 2014.

730 Cubison, M. J., Ortega, A. M., Hayes, P. L., Farmer, D. K., Day, D., Lechner, M. J., Brune, W. H., Apel, E.,
731 Diskin, G. S., Fisher, J. A., Fuelberg, H. E., Hecobian, A., Knapp, D. J., Mikoviny, T., Riemer, D.,
732 Sachse, G. W., Sessions, W., Weber, R. J., Weinheimer, A. J., Wisthaler, A., and Jimenez, J. L.:
733 Effects of aging on organic aerosol from open biomass burning smoke in aircraft and laboratory
734 studies, *Atmos. Chem. Phys.*, 11(23), 12049–12064, doi:10.5194/acp-11-12049-2011, 2011.

735 Dall’Osto, M., Paglione, M., Decesari, S., Facchini, M. C., O’Dowd, C., Plass-Duellmer, C., and Harrison, R.
736 M.: On the Origin of AMS “Cooking Organic Aerosol” at a Rural Site, *Environ. Sci. Technol.*,
737 49(24), 13964–13972, doi:10.1021/acs.est.5b02922, 2015.

738 Daumit, K. E., Kessler, S. H., and Kroll, J. H.: Average chemical properties and potential formation
739 pathways of highly oxidized organic aerosol, *Faraday Discuss.*, 165, 181,
740 doi:10.1039/c3fd00045a, 2013.

741 Decesari, S., Allan, J., Plass-Duellmer, C., Williams, B. J., Paglione, M., Facchini, M. C., O’Dowd, C.,
742 Harrison, R. M., Gietl, J. K., Coe, H., Giulianelli, L., Gobbi, G. P., Lanconelli, C., Carbone, C.,
743 Worsnop, D., Lambe, A. T., Ahern, A. T., Moretti, F., Tagliavini, E., Elste, T., Gilge, S., Zhang, Y.,
744 and Dall’Osto, M.: Measurements of the aerosol chemical composition and mixing state in the
745 Po Valley using multiple spectroscopic techniques, *Atmos. Chem. Phys.*, 14, 12109–12132,
746 doi:10.5194/acp-14-12109-2014, 2014.

747 Duplissy, J., DeCarlo, P. F., Dommen, J., Alfarra, M. R., Metzger, A., Barmapadimos, I., Prevot, A. S. H.,
748 Weingartner, E., Tritscher, T., Gysel, M., Aiken, A. C., Jimenez, J. L., Canagaratna, M. R.,
749 Worsnop, D. R., Collins, D. R., Tomlinson, J., and Baltensperger, U.: Relating hygroscopicity and
750 composition of organic aerosol particulate matter, *Atmos. Chem. Phys.*, 11(3), 1155–1165,
751 doi:10.5194/acp-11-1155-2011, 2011.

752 EC: Commission of the European communities, Commission staff working paper, Annex to the
753 communication on thematic strategy on air pollution and the directive on “Ambient air quality
754 and cleaner air for Europe”, Impact assessment, SEC (2005) 1133, available at:
755 http://ec.europa.eu/environment/archives/cafe/pdf/ia_report_en050921_final.pdf (last access:
756 15 February 2016), 2005.

757 EEA: Air quality in Europe - 2013 report, European Environment Agency (EEA), report no 9/2013,
758 publication, available at: <http://www.eea.europa.eu/publications/air-quality-in-europe-2013>
759 (last access: 15 February 2016), 2013.

760 Ervens, B., Turpin, B. J., and Weber, R. J.: Secondary organic aerosol formation in cloud droplets and
761 aqueous particles (aqSOA): a review of laboratory, field and model studies, *Atmos. Chem. Phys.*,
762 11(21), 11069–11102, doi:10.5194/acp-11-11069-2011, 2011.

763 EU: Directive 2008/50/EC of the European Parliament and of the Council of 21 May 2008 on ambient air
764 quality and cleaner air for Europe, available at [http://eur-lex.europa.eu/legal-](http://eur-lex.europa.eu/legal-content/en/ALL/?uri=CELEX:32008L0050)
765 [content/en/ALL/?uri=CELEX:32008L0050](http://eur-lex.europa.eu/legal-content/en/ALL/?uri=CELEX:32008L0050) (last access 18 July 2016), 2008.

766 Ferrero, L., Castelli, M., Ferrini, B. S., Moscatelli, M., Perrone, M. G., Sangiorgi, G., D’Angelo, L., Rovelli,
767 G., Moroni, B., Scardazza, F., Močnik, G., Bolzacchini, E., Petitta, M., and Cappelletti, D.: Impact
768 of black carbon aerosol over Italian basin valleys: high-resolution measurements along vertical
769 profiles, radiative forcing and heating rate, *Atmos. Chem. Phys.*, 14(18), 9641–9664,
770 doi:10.5194/acp-14-9641-2014, 2014.

771 Fröhlich, R., Crenn, V., Setyan, A., Belis, C. A., Canonaco, F., Favez, O., Riffault, V., Slowik, J. G., Aas, W.,
772 Aijälä, M., Alastuey, A., Artiñano, B., Bonnaire, N., Bozzetti, C., Bressi, M., Carbone, C., Coz, E.,
773 Croteau, P. L., Cubison, M. J., Esser-Gietl, J. K., Green, D. C., Gros, V., Heikkinen, L., Herrmann, H.,
774 Jayne, J. T., Lunder, C. R., Minguillón, M. C., Močnik, G., O’Dowd, C. D., Ovadnevaite, J., Petralia,
775 E., Poulain, L., Priestman, M., Ripoll, A., Sarda-Estève, R., Wiedensohler, A., Baltensperger, U.,
776 Sciare, J., and Prévôt, A. S. H.: ACTRIS ACSM intercomparison – part 2: intercomparison of ME-2
777 organic source apportionment results from 15 individual, co-located aerosol mass
778 spectrometers, *Atmos. Meas. Tech.*, 8(6), 2555–2576, doi:10.5194/amt-8-2555-2015, 2015.

779 Gaeggeler, K., Prevot, A. S. H., Dommen, J., Legreid, G., Reimann, S., and Baltensperger, U.: Residential
780 wood burning in an Alpine valley as a source for oxygenated volatile organic compounds,
781 hydrocarbons and organic acids, *Atmos. Environ.*, 42(35), 8278–8287,
782 doi:10.1016/j.atmosenv.2008.07.038, 2008.

783 Gentner, D. R., Isaacman, G., Worton, D. R., Chan, A. W. H., Dallmann, T. R., Davis, L., Liu, S., Day, D. A.,
784 Russell, L. M., Wilson, K. R., Weber, R., Guha, A., Harley, R. A., and Goldstein, A. H.: Elucidating
785 secondary organic aerosol from diesel and gasoline vehicles through detailed characterization of
786 organic carbon emissions, *Proc. Natl. Acad. Sci. USA*, 109(45), 18318–18323,
787 doi:10.1073/pnas.1212272109, 2012.

788 Gilardoni, S., Vignati, E., Cavalli, F., Putaud, J. P., Larsen, B. R., Karl, M., Stenström, K., Genberg, J.,
789 Henne, S., and Dentener, F.: Better constraints on sources of carbonaceous aerosols using a
790 combined ¹⁴C – macro tracer analysis in a European rural background site, *Atmos. Chem. Phys.*,
791 11(12), 5685–5700, doi:10.5194/acp-11-5685-2011, 2011.

792 Gilardoni, S., Massoli, P., Giulianelli, L., Rinaldi, M., Paglione, M., Pollini, F., Lanconelli, C., Poluzzi, V.,
793 Carbone, S., Hillamo, R., Russell, L. M., Facchini, M. C., and Fuzzi, S.: Fog scavenging of organic
794 and inorganic aerosol in the Po Valley, *Atmos. Chem. Phys.*, 14(13), 6967–6981,
795 doi:10.5194/acp-14-6967-2014, 2014.

796 Hand, J. L. and Kreidenweis, S. M.: A new method for retrieving particle refractive index and effective
797 density from aerosol size distribution data, *Aerosol Sci. Tech.*, 36(10), 1012–1026,
798 doi:10.1080/02786820290092276, 2002.

799 Herich, H., Gianini, M. F. D., Piot, C., Močnik, G., Jaffrezo, J.-L., Besombes, J.-L., Prévôt, A. S. H., and
800 Hueglin, C.: Overview of the impact of wood burning emissions on carbonaceous aerosols and
801 PM in large parts of the Alpine region, *Atmos. Environ.*, 89, 64–75,
802 doi:10.1016/j.atmosenv.2014.02.008, 2014.

803 Heringa, M. F., DeCarlo, P. F., Chirico, R., Tritscher, T., Dommen, J., Weingartner, E., Richter, R., Wehrle,
804 G., Prévôt, A. S. H., and Baltensperger, U.: Investigations of primary and secondary particulate
805 matter of different wood combustion appliances with a high-resolution time-of-flight aerosol
806 mass spectrometer, *Atmos. Chem. Phys.*, 11(12), 5945–5957, doi:10.5194/acp-11-5945-2011,
807 2011.

808 Hu, M., Peng, J., Sun, K., Yue, D., Guo, S., Wiedensohler, A., and Wu, Z.: Estimation of size-resolved
809 ambient particle density based on the measurement of aerosol number, mass, and chemical size
810 distributions in the winter in Beijing, *Environ. Sci. Technol.*, 120830075118007,
811 doi:10.1021/es204073t, 2012.

812 Huang, X.-F., He, L.-Y., Hu, M., Canagaratna, M. R., Sun, Y., Zhang, Q., Zhu, T., Xue, L., Zeng, L.-W., Liu, X.-
813 G., Zhang, Y.-H., Jayne, J. T., Ng, N. L., and Worsnop, D. R.: Highly time-resolved chemical
814 characterization of atmospheric submicron particles during 2008 Beijing Olympic Games using
815 an aerodyne high-resolution aerosol mass spectrometer, *Atmos. Chem. Phys.*, 10(18), 8933–
816 8945, doi:10.5194/acp-10-8933-2010, 2010.

817 Janssen, S., Ewert, F., Li, H., Athanasiadis, I. N., Wien, J. J. F., Théron, O., Knapen, M. J. R., Bezlepina, I.,
818 Alkan-Olsson, J., Rizzoli, A. E., Belhouchette, H., Svensson, M., and van Ittersum, M. K.: Defining
819 assessment projects and scenarios for policy support: use of ontology in integrated assessment
820 and modelling, *Environ. Modell. Softw.*, 24(12), 1491–1500, doi:10.1016/j.envsoft.2009.04.009,
821 2009.

822 Jayne, J. T., Leard, D. C., Zhang, X., Davidovits, P., Smith, K. A., Kolb, C. E., and Worsnop, D. R.:
823 Development of an aerosol mass spectrometer for size and composition analysis of submicron
824 particles, *Aerosol Sci. Tech.*, 33(1-2), 49–70, 2000.

825 Jimenez, J. L., Canagaratna, M. R., Donahue, N. M., Prevot, A. S. H., Zhang, Q., Kroll, J. H., DeCarlo, P. F.,
826 Allan, J. D., Coe, H., Ng, N. L., Aiken, A. C., Docherty, K. S., Ulbrich, I. M., Grieshop, A. P.,
827 Robinson, A. L., Duplissy, J., Smith, J. D., Wilson, K. R., Lanz, V. A., Hueglin, C., Sun, Y. L., Tian, J.,
828 Laaksonen, A., Raatikainen, T., Rautiainen, J., Vaattovaara, P., Ehn, M., Kulmala, M., Tomlinson,
829 J. M., Collins, D. R., Cubison, M. J., Dunlea, J., Huffman, J. A., Onasch, T. B., Alfarra, M. R.,
830 Williams, P. I., Bower, K., Kondo, Y., Schneider, J., Drewnick, F., Borrmann, S., Weimer, S.,
831 Demerjian, K., Salcedo, D., Cottrell, L., Griffin, R., Takami, A., Miyoshi, T., Hatakeyama, S.,
832 Shimojo, A., Sun, J. Y., Zhang, Y. M., Dzepina, K., Kimmel, J. R., Sueper, D., Jayne, J. T., Herndon,
833 S. C., Trimborn, A. M., Williams, L. R., Wood, E. C., Middlebrook, A. M., Kolb, C. E., Baltensperger,
834 U., and Worsnop, D. R.: Evolution of organic aerosols in the atmosphere, *Science*, 326(5959),
835 1525–1529, doi:10.1126/science.1180353, 2009.

836 Kroll, J. H., Donahue, N. M., Jimenez, J. L., Kessler, S. H., Canagaratna, M. R., Wilson, K. R., Altieri, K. E.,
837 Mazzoleni, L. R., Wozniak, A. S., Bluhm, H., Mysak, E. R., Smith, J. D., Kolb, C. E., and Worsnop, D.
838 R.: Carbon oxidation state as a metric for describing the chemistry of atmospheric organic
839 aerosol, *Nat. Chem.*, 3(2), 133–139, doi:10.1038/nchem.948, 2011.

840 Kukkonen, J., Pohjola, M., Ssokhi, R., Luhana, L., Kitwiroon, N., Fragkou, L., Rantamaki, M., Berge, E.,
841 Odegaard, V., and Havardslordal, L.: Analysis and evaluation of selected local-scale PM air
842 pollution episodes in four European cities: Helsinki, London, Milan and Oslo, *Atmos. Environ.*,
843 39(15), 2759–2773, doi:10.1016/j.atmosenv.2004.09.090, 2005.

844 Kundu, S., Kawamura, K., Andreae, T. W., Hoffer, A., and Andreae, M. O.: Molecular distributions of
845 dicarboxylic acids, ketocarboxylic acids and α -dicarbonyls in biomass burning aerosols:

846 implications for photochemical production and degradation in smoke layers, *Atmos. Chem.*
847 *Phys.*, 10(5), 2209–2225, doi:10.5194/acp-10-2209-2010, 2010.

848 Lanz, V. A., Alfarra, M. R., Baltensperger, U., Buchmann, B., Hueglin, C., and Prévôt, A. S. H.: Source
849 apportionment of submicron organic aerosols at an urban site by factor analytical modelling of
850 aerosol mass spectra, *Atmos. Chem. Phys.*, 7(6), 1503–1522, doi:10.5194/acp-7-1503-2007,
851 2007.

852 Lanz, V. A., Prévôt, A. S. H., Alfarra, M. R., Weimer, S., Mohr, C., DeCarlo, P. F., Gianini, M. F. D., Hueglin,
853 C., Schneider, J., Favez, O., D’Anna, B., George, C., and Baltensperger, U.: Characterization of
854 aerosol chemical composition with aerosol mass spectrometry in Central Europe: an overview,
855 *Atmos. Chem. Phys.*, 10(21), 10453–10471, 2010.

856 Larsen, B. R., Gilardoni, S., Stenström, K., Niedzialek, J., Jimenez, J., and Belis, C. A.: Sources for PM air
857 pollution in the Po Plain, Italy: II. Probabilistic uncertainty characterization and sensitivity
858 analysis of secondary and primary sources, *Atmos. Environ.*, 50, 203–213,
859 doi:10.1016/j.atmosenv.2011.12.038, 2012.

860 Larssen, S., Sluyter, R., and Helmig, C.: Criteria for EUROAIRNET, the EEA Air Quality Monitoring and
861 Information Network, available at:
862 http://www.eea.europa.eu/publications/TEC12/at_download/file (last access: 10 February
863 2016), 1999.

864 Lee, T., Sullivan, A. P., Mack, L., Jimenez, J. L., Kreidenweis, S. M., Onasch, T. B., Worsnop, D. R., Malm,
865 W., Wold, C. E., Hao, W. M., and Collett, J. L.: Chemical smoke marker emissions during flaming
866 and smoldering phases of laboratory open burning of wildland fuels, *Aerosol Sci. Tech.*, 44(9), i–
867 v, doi:10.1080/02786826.2010.499884, 2010.

868 Liu, P. S. K., Deng, R., Smith, K. A., Williams, L. R., Jayne, J. T., Canagaratna, M. R., Moore, K., Onasch, T.
869 B., Worsnop, D. R., and Deshler, T.: Transmission efficiency of an aerodynamic focusing lens
870 system: comparison of model calculations and laboratory measurements for the Aerodyne
871 aerosol mass spectrometer, *Aerosol Sci. Tech.*, 41(8), 721–733,
872 doi:10.1080/02786820701422278, 2007.

873 Maimone, F., Turpin, B. J., Solomon, P., Meng, Q., Robinson, A. L., Subramanian, R., and Polidori, A.:
874 Correction methods for organic carbon artifacts when using quartz-fiber filters in large
875 particulate matter monitoring networks: the regression method and other options, *J. Air Waste*
876 *Manage. Assoc.*, 61(6), 696–710, doi:10.3155/1047-3289.61.6.696, 2011.

877 McMurry, P. H., Wang, X., Park, K., and Ehara, K.: The relationship between mass and mobility for
878 atmospheric particles: a new technique for measuring particle density, *Aerosol Sci. Tech.*, 36(2),
879 227–238, doi:10.1080/027868202753504083, 2002.

880 Middlebrook, A. M., Bahreini, R., Jimenez, J. L., and Canagaratna, M. R.: Evaluation of composition-
881 dependent collection efficiencies for the Aerodyne aerosol mass spectrometer using field data,
882 *Aerosol Sci. Tech.*, 46(3), 258–271, doi:10.1080/02786826.2011.620041, 2012.

883 Miljevic, B., Heringa, M. F., Keller, A., Meyer, N. K., Good, J., Lauber, A., Decarlo, P. F., Fairfull-Smith, K.
884 E., Nussbaumer, T., Burtscher, H., Prévôt, A. S. H., Baltensperger, U., Bottle, S. E., and Ristovski,
885 Z. D.: Oxidative potential of logwood and pellet burning particles assessed by a novel
886 profluorescent nitroxide probe, *Environ. Sci. Technol.*, 44(17), 6601–6607, 2010.

887 Minguillón, M. C., Ripoll, A., Pérez, N., Prévôt, A. S. H., Canonaco, F., Querol, X., and Alastuey, A.:
888 Chemical characterization of submicron regional background aerosols in the western
889 Mediterranean using an aerosol chemical speciation monitor, *Atmos. Chem. Phys.*, 15(11),
890 6379–6391, doi:10.5194/acp-15-6379-2015, 2015.

891 Naeher, L. P., Brauer, M., Lipsett, M., Zelikoff, J. T., Simpson, C. D., Koenig, J. Q., and Smith, K. R.:
892 Woodsmoke health effects: a review, *Inhal. Toxicol.*, 19(1), 67–106,
893 doi:10.1080/08958370600985875, 2007.

894 Ng, N. L., Herndon, S. C., Trimborn, A., Canagaratna, M. R., Croteau, P. L., Onasch, T. B., Sueper, D.,
895 Worsnop, D. R., Zhang, Q., Sun, Y. L., and Jayne, J. T.: An aerosol chemical speciation monitor
896 (ACSM) for routine monitoring of the composition and mass concentrations of ambient aerosol,
897 *Aerosol Sci. Tech.*, 45(7), 780–794, doi:10.1080/02786826.2011.560211, 2011a.

898 Ng, N. L., Canagaratna, M. R., Jimenez, J. L., Chhabra, P. S., Seinfeld, J. H., and Worsnop, D. R.: Changes in
899 organic aerosol composition with aging inferred from aerosol mass spectra, *Atmos. Chem. Phys.*,
900 11(13), 6465–6474, doi:10.5194/acp-11-6465-2011, 2011b.

901 Ng, N. L., Canagaratna, M. R., Jimenez, J. L., Zhang, Q., Ulbrich, I. M., and Worsnop, D. R.: Real-time
902 methods for estimating organic component mass concentrations from aerosol mass
903 spectrometer data, *Environ. Sci. Technol.*, 45(3), 910–916, doi:10.1021/es102951k, 2011c.

904 Paatero, P.: User's guide for the multilinear engine program "ME2" for fitting multilinear and
905 quasimultilinear models, University of Helsinki, Finland, 2000.

906 Paatero, P. and Tapper, U.: Positive matrix factorization - a nonnegative factor model with optimal
907 utilization of error-estimates of data values, *Environmetrics*, 5(2), 111–126,
908 doi:10.1002/env.3170050203, 1994.

909 Paglione, M., Saarikoski, S., Carbone, S., Hillamo, R., Facchini, M. C., Finessi, E., Giulianelli, L., Carbone,
910 C., Fuzzi, S., Moretti, F., Tagliavini, E., Swietlicki, E., Eriksson Stenström, K., Prévôt, A. S. H.,
911 Massoli, P., Canaragatna, M., Worsnop, D., and Decesari, S.: Primary and secondary biomass
912 burning aerosols determined by proton nuclear magnetic resonance (¹H-NMR) spectroscopy
913 during the 2008 EUCAARI campaign in the Po Valley (Italy), *Atmos. Chem. Phys.*, 14(10), 5089–
914 5110, doi:10.5194/acp-14-5089-2014, 2014.

915 Pernigotti, D., Georgieva, E., Thunis, P., and Bessagnet, B.: Impact of meteorology on air quality
916 modeling over the Po valley in northern Italy, *Atmos. Environ.*, 51, 303–310,
917 doi:10.1016/j.atmosenv.2011.12.059, 2012.

918 Perrone, M. G., Larsen, B. R., Ferrero, L., Sangiorgi, G., De Gennaro, G., Udisti, R., Zangrando, R.,
919 Gambaro, A., and Bolzacchini, E.: Sources of high PM_{2.5} concentrations in Milan, northern Italy:
920 molecular marker data and CMB modelling, *Sci. Total Environ.*, 414, 343–355,
921 doi:10.1016/j.scitotenv.2011.11.026, 2012.

922 Petit, J.-E., Favez, O., Sciare, J., Crenn, V., Sarda-Estève, R., Bonnaire, N., Močnik, G., Dupont, J.-C.,
923 Haeffelin, M., and Leoz-Garziandia, E.: Two years of near real-time chemical composition of
924 submicron aerosols in the region of Paris using an aerosol chemical speciation monitor (ACSM)
925 and a multi-wavelength aethalometer, *Atmos. Chem. Phys.*, 15, 2985–3005, doi:10.5194/acp-15-
926 2985-2015, 2015.

927 Pitz, M., Cyrus, J., Karg, E., Wiedensohler, A., Wichmann, H.-E., and Heinrich, J.: Variability of apparent
928 particle density of an urban aerosol, *Environ. Sci. Technol.*, 37(19), 4336–4342,
929 doi:10.1021/es034322p, 2003.

930 Pitz, M., Schmid, O., Heinrich, J., Birmili, W., Maguhn, J., Zimmermann, R., Wichmann, H.-E., Peters, A.,
931 and Cyrus, J.: Seasonal and diurnal variation of PM_{2.5} apparent particle density in urban air in
932 Augsburg, Germany, *Environ. Sci. Technol.*, 42(14), 5087–5093, 2008.

933 Putaud, J. P., Van Dingenen, R., and Raes, F.: Submicron aerosol mass balance at urban and semirural
934 sites in the Milan area (Italy), *J. Geophys. Res.-Atmos.*, 107(D22), LOP 11–1–LOP 11–10,
935 doi:10.1029/2000JD000111, 2002.

936 Putaud, J.-P., Van Dingenen, R., Alastuey, A., Bauer, H., Birmili, W., Cyrus, J., Flentje, H., Fuzzi, S., Gehrig,
937 R., Hansson, H. C., Harrison, R. M., Herrmann, H., Hitzenberger, R., Hüglin, C., Jones, A. M.,
938 Kasper-Giebl, A., Kiss, G., Kousa, A., Kuhlbusch, T. A. J., Loschau, G., Maenhaut, W., Molnar, A.,
939 Moreno, T., Pekkanen, J., Perrino, C., Pitz, M., Puxbaum, H., Querol, X., Rodriguez, S., Salma, I.,
940 Schwarz, J., Smolik, J., Schneider, J., Spindler, G., ten Brink, H., Tursic, J., Viana, M.,
941 Wiedensohler, A., and Raes, F.: A European aerosol phenomenology – 3: physical and chemical

942 characteristics of particulate matter from 60 rural, urban, and kerbside sites across Europe,
943 *Atmos. Environ.*, 44, 1308–1320, 2010.

944 Putaud, J.-P., Adam, M., Belis, C. A., Bergamaschi, P., Cancellinha, J., Cavalli, F., Cescatti, A., Daou, D.,
945 Dell’Acqua, A., Douglas, K., Duerr, M., Goded, I., Grassi, F., Gruening, C., Hjorth, J., Jensen, N. R.,
946 Lagler, F., Manca, G., Martins Dos Santos, S., Passarella, R., Pedroni, V., Rocha e Abreu, P., Roux,
947 D., Scheeren, B., and Schembari, C.: JRC-Ispira Atmosphere-Biosphere-Climate Integrated
948 monitoring Station (ABC-IS): 2011 report, JRC Technical Reports, Joint Research Centre, Ispra
949 (Italy), available at:
950 [http://publications.jrc.ec.europa.eu/repository/bitstream/111111111/28242/1/lb-na-25753-en-](http://publications.jrc.ec.europa.eu/repository/bitstream/111111111/28242/1/lb-na-25753-en-n.pdf)
951 [n.pdf](http://publications.jrc.ec.europa.eu/repository/bitstream/111111111/28242/1/lb-na-25753-en-n.pdf) (last access: 28 March 2014), 2013.

952 Putaud, J.-P., Bergamaschi, P., Bressi, M., Cavalli, F., Cescatti, A., Daou, D., Dell’acqua, A., Douglas, K.,
953 Duerr, M., Fumagalli, I., Goded Ballarin, I., Grassi, F., Gruening, C., Hjorth, J., Jensen, N., Lagler,
954 F., Manca, G., Martins Dos Santos, S., Matteucci, M., Passarella, R., Pedroni, V., Pokorska, O.,
955 and Roux, D.: JRC – Ispra Atmosphere – Biosphere – Climate Integrated monitoring Station 2013
956 report, EUR - Scientific and Technical Research Reports, Publications Office of the European
957 Union, available at: <http://publications.jrc.ec.europa.eu/repository/handle/111111111/33904>
958 (last access: 19 February 2015), 2014a.

959 Putaud, J. P., Cavalli, F., Martins dos Santos, S., and Dell’Acqua, A.: Long-term trends in aerosol optical
960 characteristics in the Po Valley, Italy, *Atmos. Chem. Phys.*, 14(17), 9129–9136, doi:10.5194/acp-
961 14-9129-2014, 2014b.

962 Reiss, R., Anderson, E. L., Cross, C. E., Hidy, G., Hoel, D., McClellan, R., and Moolgavkar, S.: Evidence of
963 health impacts of sulfate- and nitrate-containing particles in ambient air, *Inhal. Toxicol.*, 19(5),
964 419–449, doi:10.1080/08958370601174941, 2007.

965 Riffault, V., Zhang, S., Tison, E., and Setyan, A.: Chloride RIE measurements, 14th AMS user meeting, 8
966 September 2013, available at: [http://cires.colorado.edu/jimenez-](http://cires.colorado.edu/jimenez-group/UsrMtgs/UsersMtg14/AMS_user_meeting_ChI_RIE_riffault.pdf)
967 [group/UsrMtgs/UsersMtg14/AMS_user_meeting_ChI_RIE_riffault.pdf](http://cires.colorado.edu/jimenez-group/UsrMtgs/UsersMtg14/AMS_user_meeting_ChI_RIE_riffault.pdf) (last access: 10 February
968 2016), 2013.

969 Ripoll, A., Minguillón, M. C., Pey, J., Jimenez, J. L., Day, D. A., Sosedova, Y., Canonaco, F., Prévôt, A. S. H.,
970 Querol, X., and Alastuey, A.: Long-term real-time chemical characterization of submicron
971 aerosols at Montsec (southern Pyrenees, 1570 m a.s.l.), *Atmos. Chem. Phys.*, 15(6), 2935–2951,
972 doi:10.5194/acp-15-2935-2015, 2015.

973 Saarikoski, S., Carbone, S., Decesari, S., Giulianelli, L., Angelini, F., Canagaratna, M., Ng, N. L., Trimborn,
974 A., Facchini, M. C., Fuzzi, S., Hillamo, R., and Worsnop, D.: Chemical characterization of
975 springtime submicrometer aerosol in Po Valley, Italy, *Atmos. Chem. Phys.*, 12(18), 8401–8421,
976 doi:10.5194/acp-12-8401-2012, 2012.

977 Schaap, M., Van Loon, M., Ten Brink, H. M., Dentener, F. J., and Builtjes, P. J. H.: Secondary inorganic
978 aerosol simulations for Europe with special attention to nitrate, *Atmos. Chem. Phys.*, 4(3), 857–
979 874, 2004.

980 Schlesinger, R. B. and Cassee, F.: Atmospheric secondary inorganic particulate matter: the toxicological
981 perspective as a basis for health effects risk assessment, *Inhal. Toxicol.*, 15(3), 197–235,
982 doi:10.1080/08958370390168247, 2003.

983 Seinfeld, J. H. and Pandis, S. N.: *Atmospheric Chemistry and Physics: from Air Pollution to Climate*
984 *Change*, Wiley, New York, USA, 2006.

985 Sturtz, T. M., Adar, S. D., Gould, T., and Larson, T. V.: Constrained source apportionment of coarse
986 particulate matter and selected trace elements in three cities from the multi-ethnic study of
987 atherosclerosis, *Atmos. Environ.*, 84, 65–77, doi:10.1016/j.atmosenv.2013.11.031, 2014.

988 Sun, Y., Wang, Z., Dong, H., Yang, T., Li, J., Pan, X., Chen, P., and Jayne, J. T.: Characterization of summer
989 organic and inorganic aerosols in Beijing, China with an aerosol chemical speciation monitor,
990 *Atmos. Environ.*, 51, 250–259, doi:10.1016/j.atmosenv.2012.01.013, 2012.

991 Takegawa, N., Miyazaki, Y., Kondo, Y., Komazaki, Y., Miyakawa, T., Jimenez, J. L., Jayne, J. T., Worsnop, D.
992 R., Allan, J. D., and Weber, R. J.: Characterization of an Aerodyne aerosol mass spectrometer
993 (AMS): intercomparison with other aerosol instruments, *Aerosol Sci. Tech.*, 39(8), 760–770,
994 doi:10.1080/02786820500243404, 2005.

995 Takegawa, N., Miyakawa, T., Kondo, Y., Jimenez, J. L., Zhang, Q., Worsnop, D. R., and Fukuda, M.:
996 Seasonal and diurnal variations of submicron organic aerosol in Tokyo observed using the
997 Aerodyne aerosol mass spectrometer, *J. Geophys. Res.-Atmos.*, 111(D11), D11206,
998 doi:10.1029/2005JD006515, 2006.

999 Turpin, B. J. and Lim, H. J.: Species contributions to PM_{2.5} mass concentrations: revisiting common
1000 assumptions for estimating organic mass, *Aerosol Sci. Tech.*, 35(1), 602–610,
1001 doi:10.1080/02786820152051454, 2001.

1002 Turpin, B. J., Saxena, P., and Andrews, E.: Measuring and simulating particulate organics in the
1003 atmosphere: problems and prospects, *Atmos. Environ.*, 34(18), 2983–3013, 2000.

1004 Ulbrich, I. M., Canagaratna, M. R., Zhang, Q., Worsnop, D. R., and Jimenez, J. L.: Interpretation of organic
1005 components from positive matrix factorization of aerosol mass spectrometric data, *Atmos.*
1006 *Chem. Phys.*, 9(9), 2891–2918, 2009.

1007 Ulbrich, I. M., Lechner, M., and Jimenez, J. L.: AMS Spectral Database, available at:
1008 <http://cires.colorado.edu/jimenez-group/AMSsd/> (last access: 7 October 2015), 2015.

1009 van Donkelaar, A., Martin, R. V., Brauer, M., Kahn, R., Levy, R., Verduzco, C., and Villeneuve, P. J.: Global
1010 estimates of ambient fine particulate matter concentrations from satellite-based aerosol optical
1011 depth: development and application, *Environ. Health Persp.*, 118(6), 847–855,
1012 doi:10.1289/ehp.0901623, 2010.

1013 Volkamer, R., Jimenez, J. L., San Martini, F., Dzepina, K., Zhang, Q., Salcedo, D., Molina, L. T., Worsnop, D.
1014 R., and Molina, M. J.: Secondary organic aerosol formation from anthropogenic air pollution:
1015 rapid and higher than expected, *Geophys. Res. Lett.*, 33(17), doi:10.1029/2006GL026899, 2006.

1016 Watson, J. G., Chow, J. C., Chen, L.-W. A., and Frank, N. H.: Methods to assess carbonaceous aerosol
1017 sampling artifacts for IMPROVE and other long-term networks, *J. Air Waste Manage. Assoc.*,
1018 59(8), 898–911, doi:10.3155/1047-3289.59.8.898, 2009.

1019 Weimer, S., Drewnick, F., Högrefe, O., Schwab, J. J., Rhoads, K., Orsini, D., Canagaratna, M., Worsnop, D.
1020 R., and Demerjian, K. L.: Size-selective nonrefractory ambient aerosol measurements during the
1021 particulate matter technology assessment and characterization study - New York 2004 winter
1022 intensive in New York City, *J. Geophys. Res.*, 111(D18), doi:10.1029/2006JD007215, 2006.

1023 WHO: WHO Air quality guidelines for particulate matter, ozone, nitrogen dioxide and sulfur dioxide:
1024 global update 2005: summary of risk assessment, available at:
1025 <http://apps.who.int/iris/handle/10665/69477> (last access: 10 October 2014), 2006.

1026 WHO: Review of evidence on health aspects of air pollution_ REVIHAAP Project, Technical Report,
1027 available at: [http://www.euro.who.int/__data/assets/pdf_file/0004/193108/REVIHAAP-Final-](http://www.euro.who.int/__data/assets/pdf_file/0004/193108/REVIHAAP-Final-technical-report-final-version.pdf)
1028 [technical-report-final-version.pdf](http://www.euro.who.int/__data/assets/pdf_file/0004/193108/REVIHAAP-Final-technical-report-final-version.pdf) (last access: 15 April 2015), 2013.

1029 Wiedensohler, A., Birmili, W., Nowak, A., Sonntag, A., Weinhold, K., Merkel, M., Wehner, B., Tuch, T.,
1030 Pfeifer, S., Fiebig, M., Fjåraa, A. M., Asmi, E., Sellegri, K., Depuy, R., Venzac, H., Villani, P., Laj, P.,
1031 Aalto, P., Ogren, J. A., Swietlicki, E., Williams, P., Roldin, P., Quincey, P., Hüglin, C., Fierz-
1032 Schmidhauser, R., Gysel, M., Weingartner, E., Riccobono, F., Santos, S., Grüning, C., Faloon, K.,
1033 Beddows, D., Harrison, R., Monahan, C., Jennings, S. G., O’Dowd, C. D., Marinoni, A., Horn, H.-G.,
1034 Keck, L., Jiang, J., Scheckman, J., McMurry, P. H., Deng, Z., Zhao, C. S., Moerman, M., Henzing, B.,
1035 de Leeuw, G., Lösschau, G., and Bastian, S.: Mobility particle size spectrometers: harmonization

1036 of technical standards and data structure to facilitate high quality long-term observations of
1037 atmospheric particle number size distributions, *Atmos. Meas. Tech.*, 5(3), 657–685,
1038 doi:10.5194/amt-5-657-2012, 2012.

1039 WMO, Zhu, T., Melamed, M., Parrish, D., Gauss, M., Gallardo Klenner, L., Lawrence, M., Konare, A., and
1040 Lioussé, C.: WMO/IGAC impacts of megacities on air pollution and climate, available at:
1041 http://www.igacproject.org/sites/all/themes/bluemasters/images/GAW_Report_205.pdf (last
1042 access: 29 July 2015), 2012.

1043 Young, D. E., Allan, J. D., Williams, P. I., Green, D. C., Harrison, R. M., Yin, J., Flynn, M. J., Gallagher, M.
1044 W., and Coe, H.: Investigating a two-component model of solid fuel organic aerosol in London:
1045 processes, PM₁ contributions, and seasonality, *Atmos. Chem. Phys.*, 15(5), 2429–2443,
1046 doi:10.5194/acp-15-2429-2015, 2015.

1047 Zhang, Q.: Time- and size-resolved chemical composition of submicron particles in Pittsburgh:
1048 implications for aerosol sources and processes, *J. Geophys. Res.*, 110(D7),
1049 doi:10.1029/2004JD004649, 2005.

1050 Zhang, Q., Jimenez, J. L., Canagaratna, M. R., Allan, J. D., Coe, H., Ulbrich, I., Alfarra, M. R., Takami, A.,
1051 Middlebrook, A. M., Sun, Y. L., Dzepina, K., Dunlea, E., Docherty, K., DeCarlo, P. F., Salcedo, D.,
1052 Onasch, T., Jayne, J. T., Miyoshi, T., Shimojo, A., Hatakeyama, S., Takegawa, N., Kondo, Y.,
1053 Schneider, J., Drewnick, F., Borrmann, S., Weimer, S., Demerjian, K., Williams, P., Bower, K.,
1054 Bahreini, R., Cottrell, L., Griffin, R. J., Rautiainen, J., Sun, J. Y., Zhang, Y. M., and Worsnop, D. R.:
1055 Ubiquity and dominance of oxygenated species in organic aerosols in anthropogenically-
1056 influenced Northern Hemisphere midlatitudes, *Geophys. Res. Lett.*, 34(13),
1057 doi:10.1029/2007GL029979, 2007.

1058 Zhang, Q., Jimenez, J. L., Canagaratna, M. R., Ulbrich, I. M., Ng, N. L., Worsnop, D. R., and Sun, Y.:
1059 Understanding atmospheric organic aerosols via factor analysis of aerosol mass spectrometry: a
1060 review, *Anal. Bioanal. Chem.*, 401(10), 3045–3067, doi:10.1007/s00216-011-5355-y, 2011.

1061 **Tables and Figures**

1062

1063 Table 1. Consistency of ACSM measurements: comparison between ACSM and independent analytical techniques using orthogonal regression
 1064 analyses. Slopes and intercepts are indicated \pm uncertainties.

1065

	r^2					slope					intercept				
	Sp	Su	Au	Wi	An	Sp	Su	Au	Wi	An	Sp	Su	Au	Wi	An
Org vs OC	0.91	0.90	0.86	0.92	0.77	2.18 \pm 0.07	2.92 \pm 0.10	1.87 \pm 0.09	1.26 \pm 0.04	1.72 \pm 0.04	-0.29 \pm 0.37	-1.07 \pm 0.32	-0.28 \pm 0.36	0.74 \pm 0.37	0.61 \pm 0.25
Nitrate	0.95	0.53	0.96	0.92	0.91	1.37 \pm 0.03	4.27 \pm 0.25	1.28 \pm 0.03	0.86 \pm 0.03	1.28 \pm 0.02	0.42 \pm 0.18	0.64 \pm 0.11	0.48 \pm 0.10	0.62 \pm 0.11	0.48 \pm 0.09
Sulfate	0.96	0.97	0.92	0.86	0.95	1.05 \pm 0.02	0.98 \pm 0.02	0.96 \pm 0.04	1.38 \pm 0.06	1.00 \pm 0.01	-0.01 \pm 0.04	0.02 \pm 0.06	0.04 \pm 0.07	-0.25 \pm 0.06	0.00 \pm 0.03
Ammonium	0.92	0.70	0.91	0.95	0.90	1.03 \pm 0.03	1.00 \pm 0.06	0.93 \pm 0.04	0.81 \pm 0.02	0.99 \pm 0.02	-0.04 \pm 0.07	-0.04 \pm 0.07	-0.12 \pm 0.05	0.03 \pm 0.03	-0.08 \pm 0.03
Chloride	0.75	0.00	0.59	0.78	0.52	2.68 \pm 0.13	-0.13 \pm 0.09	0.68 \pm 0.06	1.13 \pm 0.07	1.75 \pm 0.06	0.04 \pm 0.01	0.03 \pm 0.00	0.04 \pm 0.00	-0.02 \pm 0.01	0.02 \pm 0.01
Mass vs volume	0.87	0.82	0.88	0.85	0.81	1.91 \pm 0.01	1.95 \pm 0.02	1.45 \pm 0.01	1.34 \pm 0.01	1.63 \pm 0.01	-1.16 \pm 0.19	-1.36 \pm 0.18	-2.45 \pm 0.19	-0.11 \pm 0.20	-1.09 \pm 0.11

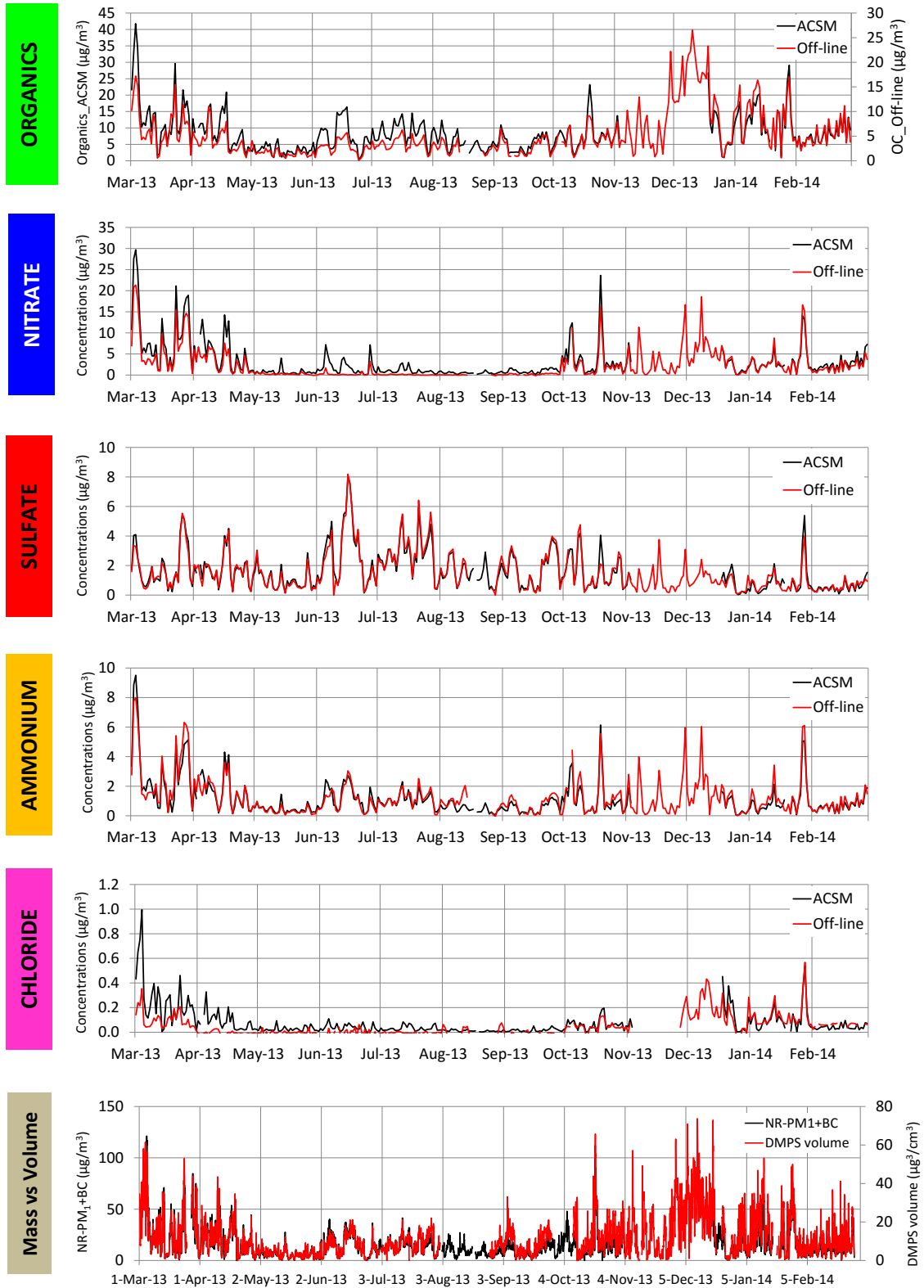
1066

1067 Legend: Sp: spring (March-April-May), Su: summer (June-July-August), Au: autumn (September-October-November), Wi: winter (December-
 1068 January-February), An: annual. Independent analytical techniques refer to i) EC-OC Sunset Analyzer for OC from PM_{2.5} sampling, ii) Ion
 1069 Chromatography for ions from PM_{2.5} sampling and iii) DMPS for volume concentrations (see Sect. 2.3 for more details). Mass refers to NR-
 1070 PM₁+BC. Intercepts are in $\mu\text{g}/\text{m}^3$. Slopes are in g/cm^3 for mass vs volume and dimensionless otherwise.

1071 Table 2. Comparison (coefficient of determination, r^2) between SA factors, organic m/z tracers and independent species time series. BC stands
 1072 for Black Carbon; Org_i stands for organic signal at m/z i (i=43, 44, 60, 67, 73, 81).

1073

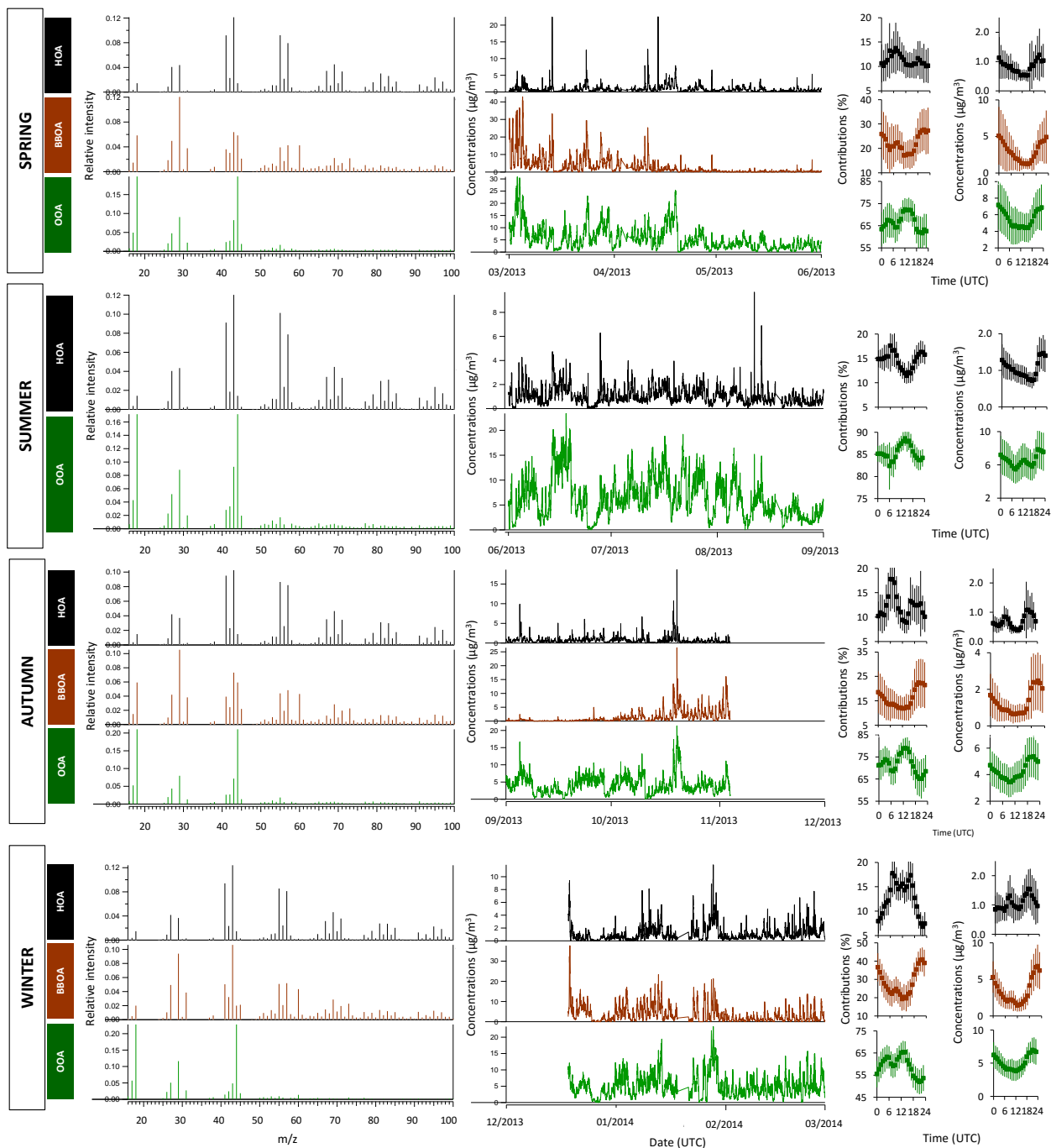
	HOA					BBOA					OOA				
	Org_67	Org_81	NOx	CO	BC	Org_60	Org_73	NOx	CO	BC	Org_43	Org_44	NH4	SO4	NO3
SPRING	0.60	0.55	0.03	0.08	0.28	0.99	0.97	0.32	0.81	0.70	0.88	0.94	0.76	0.43	0.77
SUMMER	0.90	0.91	0.07	0.40	0.52			-			0.97	0.94	0.54	0.60	0.19
AUTUMN	0.63	0.61	0.07	0.10	0.24	0.99	0.97	0.06	0.68	0.47	0.82	0.92	0.47	0.53	0.38
WINTER	0.58	0.57	0.34	0.33	0.39	0.98	0.97	0.20	0.66	0.63	0.80	0.99	0.50	0.39	0.66



1074

1075 Figure 1. Comparison between measurements performed with the ACSM and other co-located analytical

1076 techniques. See Table 1 and Sect. 2.3 for more details.

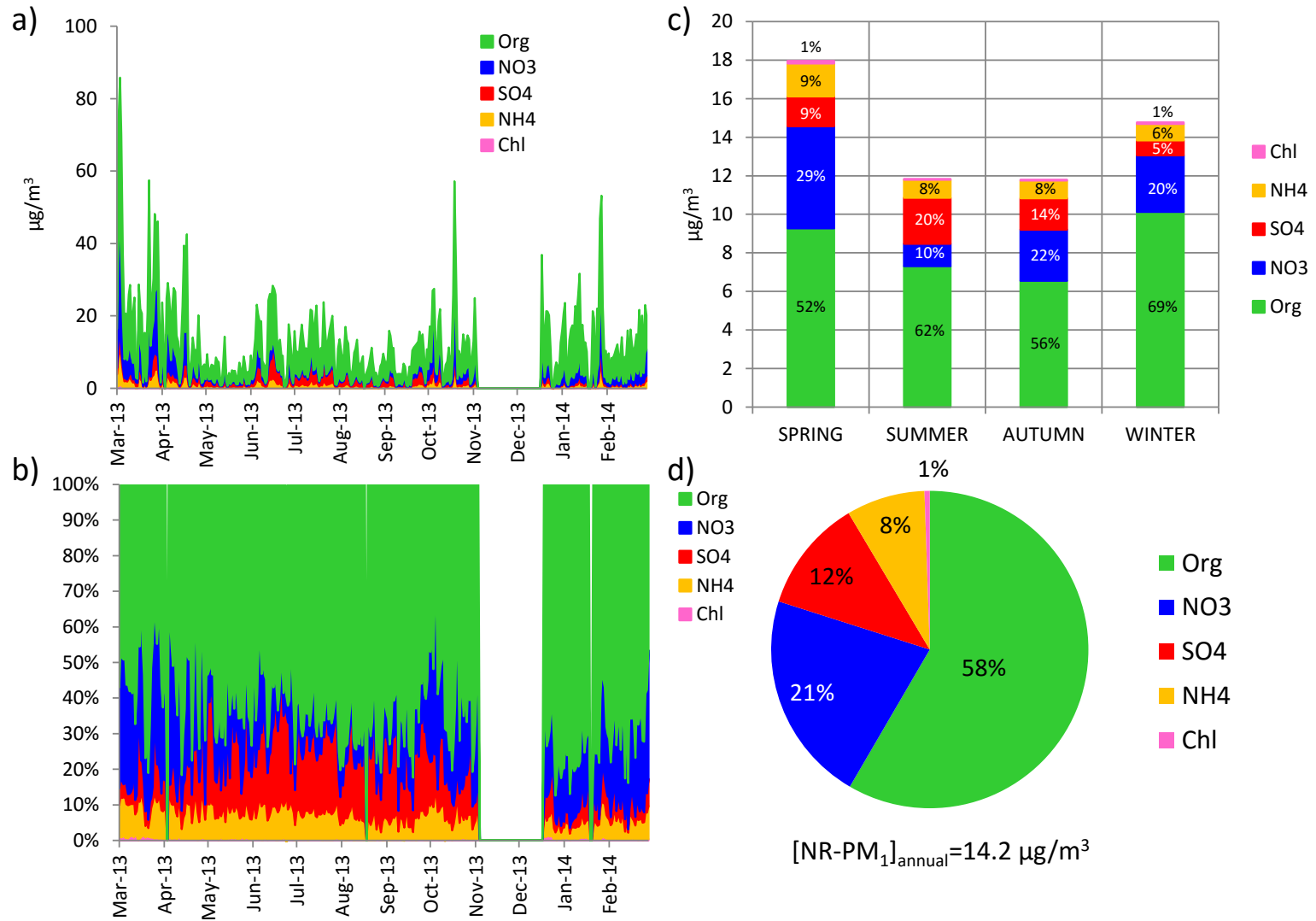


1077

1078 Figure 2. Organic source apportionment presented by season: factor profiles (left), time series (middle)

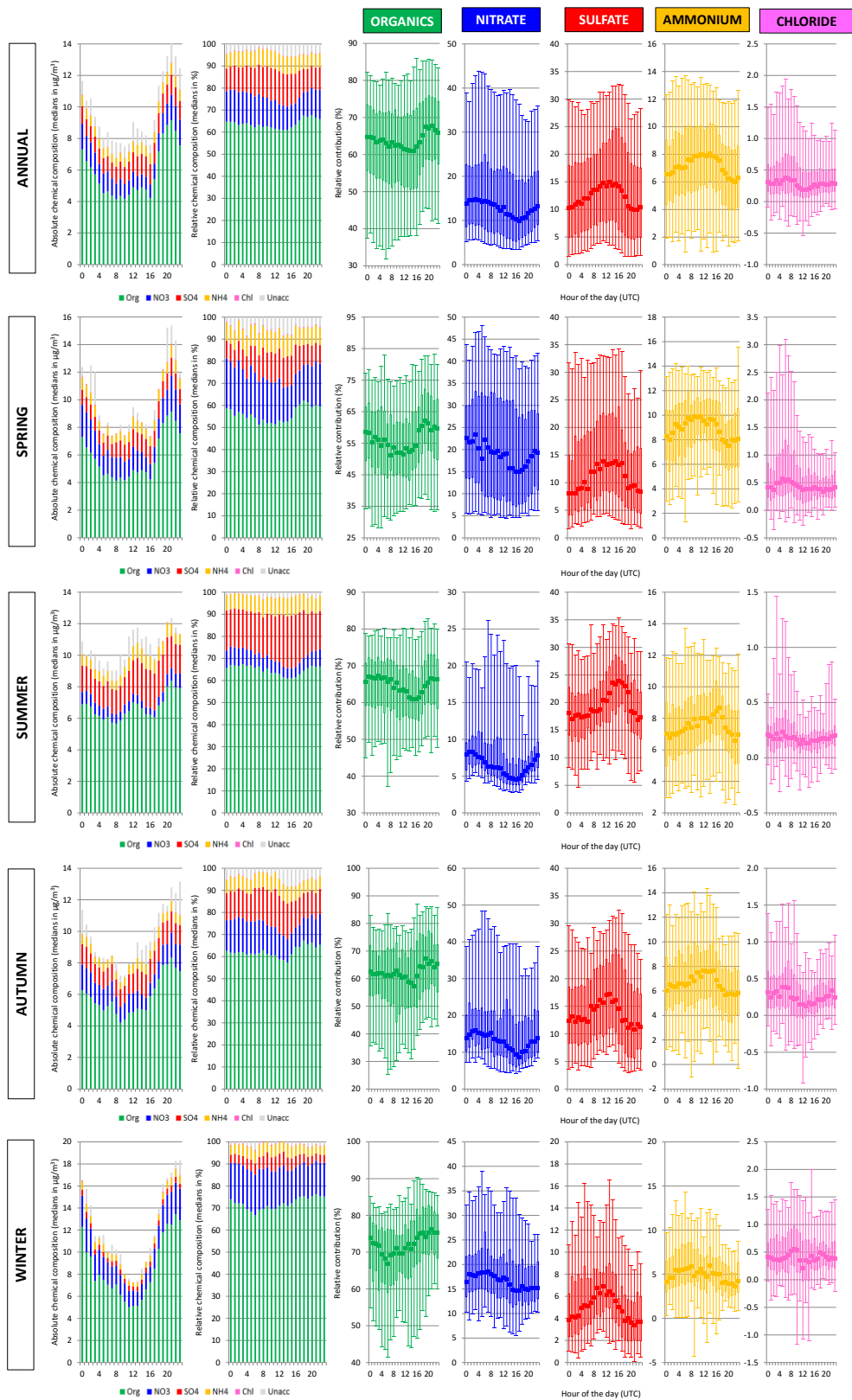
1079 and daily cycles (right, error bars represent 1 standard deviation). Seasons are defined as Spring: MAM,

1080 Summer: JJA, Autumn: SON and Winter: DJF.



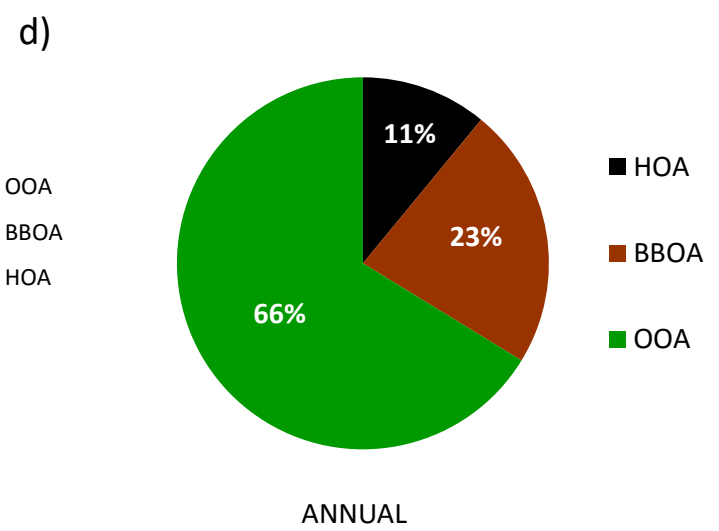
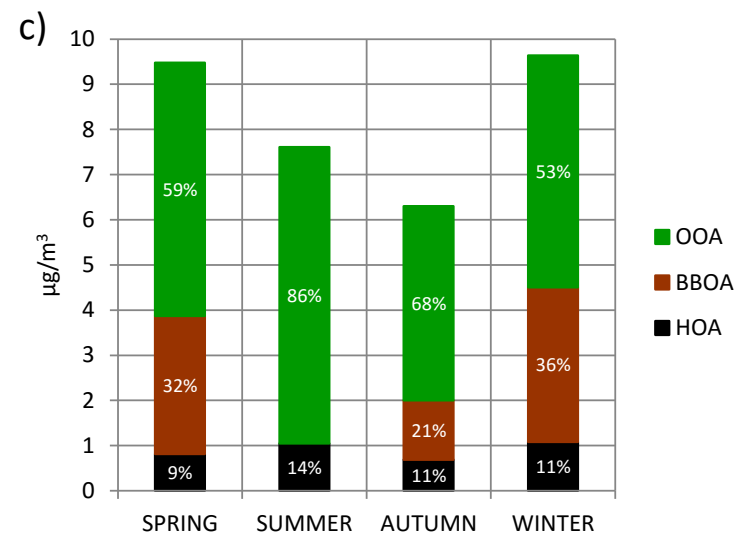
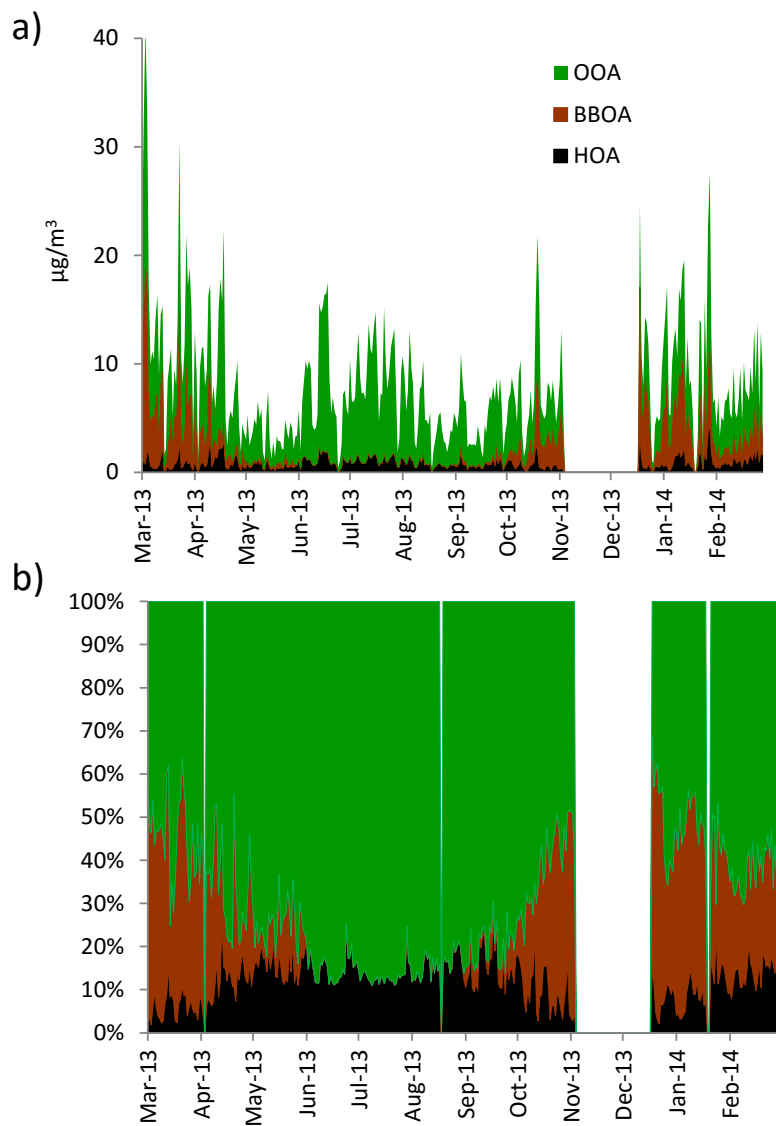
1081

1082 Figure 3. Overview of the chemical composition of NR-PM₁ at Ispra (Po Valley, Italy): daily absolute (a) and relative (b) chemical composition;
 1083 seasonal (c) and annual (d) averages.



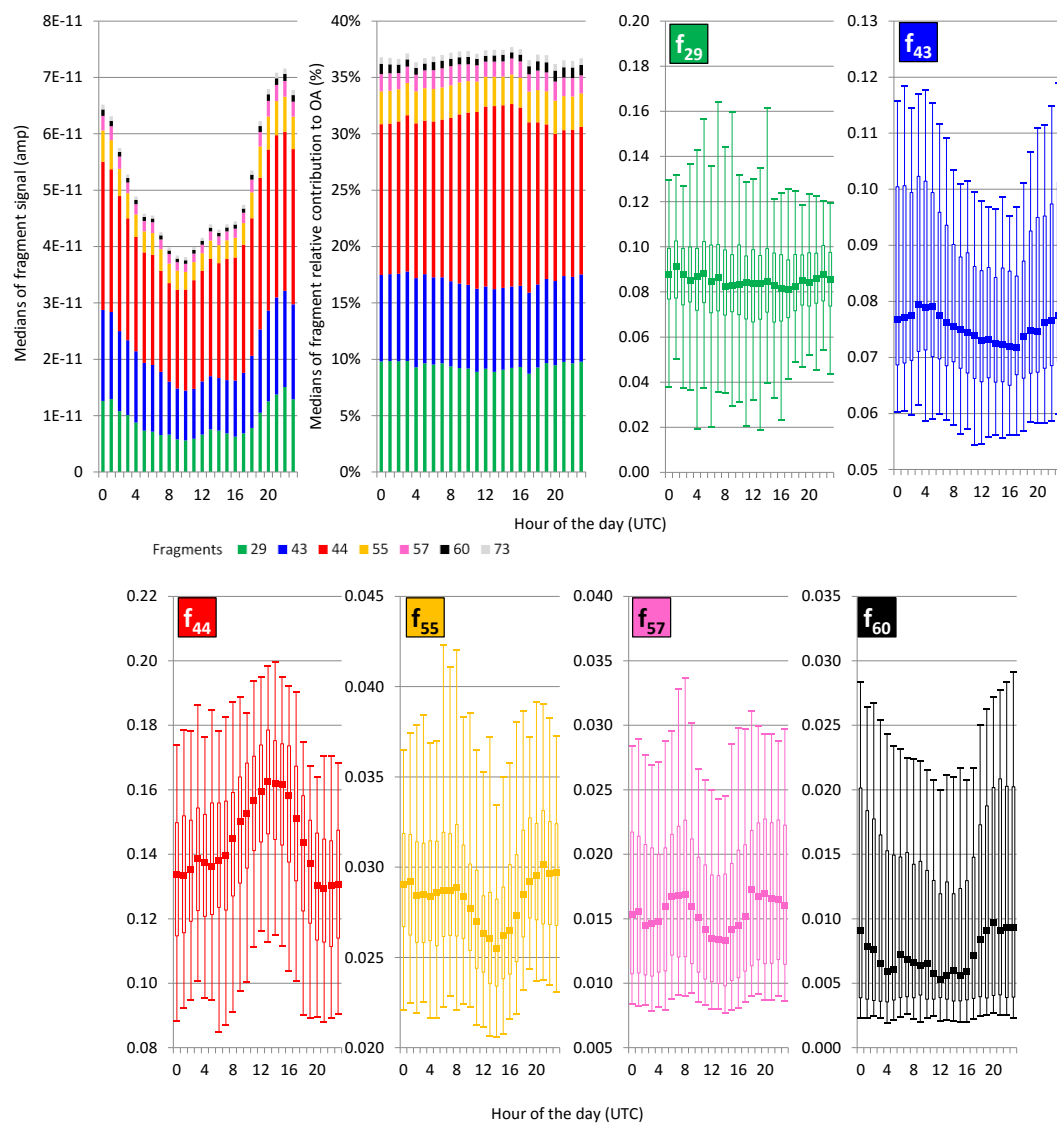
1084

1085 Figure 4. Daily cycles of NR-PM₁ chemical composition on the annual and seasonal scales. Unacc:
 1086 unaccounted mass, whisker plots are constructed from the 5th, 25th, 50th, 75th and 95th percentiles.



1087

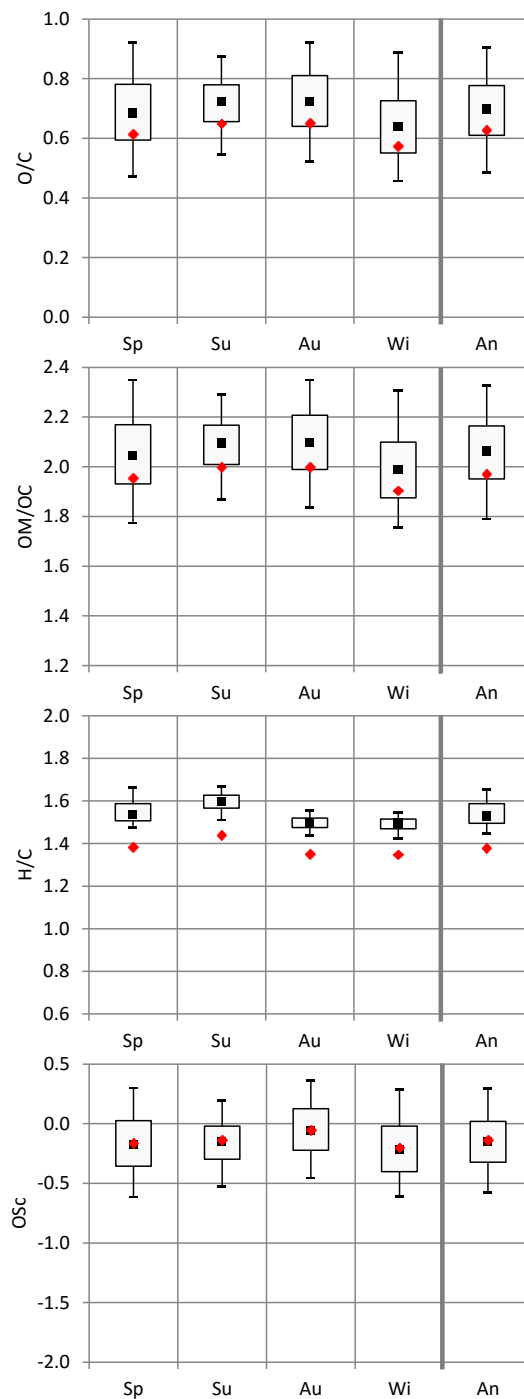
1088 Figure 5. Overview of HOA, BBOA and OOA contributions to organic aerosols; see legend Figure 3.



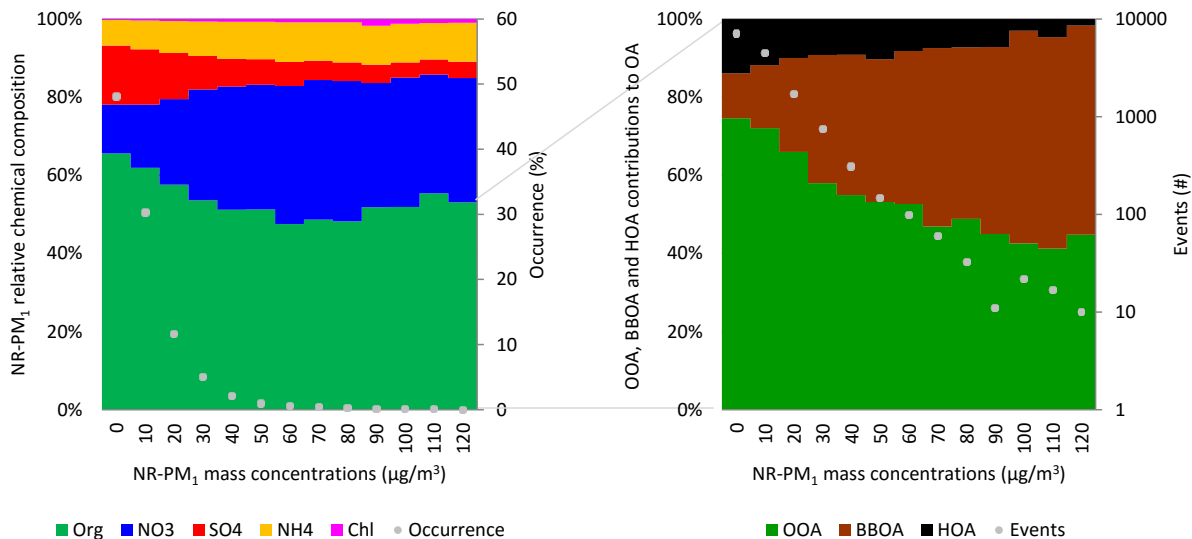
1089

1090 Figure 6. Annual statistics describing the daily cycles of the major organic fragments. Box plots are constructed from the 5th, 25th, 50th, 75th and

1091 95th percentiles.



1092
 1093 Figure 7. Seasonal and annual O/C, OM/OC, H/C and OSc of ambient OA. Sp: spring (MAM), Su: summer
 1094 (JJA), Au: autumn (SON), Wi: winter (DJF), An: annual. Black: 5th, 25th, 50th, 75th and 95th percentiles
 1095 estimates following Canagaratna et al. (2015); red: median estimates following Aiken et al. (2008) for
 1096 O/C and OM/C, Ng et al. (2011b) for H/C and Aiken et al. (2008), Kroll et al. (2011) and Ng et al. (2011b)
 1097 for OSc. Note that the authors do not recommend comparing absolute O/C, OM/OC and OSc values
 1098 reported here with other AMS studies, given the uncertainties associated with f_{44} quantifications from
 1099 ACSM measurements (please see text).



1100

1101 Figure 8. NR-PM₁ relative chemical composition (left) and OA factor contributions (right) averages as a
 1102 function of NR-PM₁ mass concentrations (bins of 10 μg/m³). Occurrence (%), left) and number of
 1103 pollution events (#, right) are indicated (solid dots) for each NR-PM₁ bin. Note that one event
 1104 corresponds to one 30 minute average.